https://doi.org/10.1016/j.buildenv.2015.09.030

Indirect evaporative cooler considering condensation from primary air: model development and parameter analysis

Yi CHEN, Hongxing YANG*, Yimo LUO

Renewable Energy Research Group (RERG), Department of Building Services Engineering, The Hong Kong Polytechnic University, Hong Kong

Abstract

The indirect evaporative cooler (IEC), regarded as a low-carbon cooling device, was proposed as fresh air pre-cooling and heat recovery device in the air-conditioning system to break the region limitation of application in hot and humid areas. In this hybrid system, the exhausted air with low temperature and humidity from air-conditioned space is used as secondary air to cool the inlet fresh air. As the dew point temperature of the fresh air is high, condensation may occur in the dry channels. However, the modeling of IEC with condensation has been seldom studied and corresponding parameter study is also lacking. So the paper established a new numerical model taking the condensation from primary air into consideration. The model was validated by the published data from literatures with good agreement. Nine parameters were analyzed in detail under three operation states (non-condensation, partially condensation and totally condensation) using four evaluation indexes: condensation ratio, wet-bulb efficiency, enlargement coefficient and total heat transfer rate. The results show that the condensation lowers the wet-bulb efficiency of IEC but improves the total heat transfer rate due to dehumidification.

Keywords: indirect evaporative cooler, condensation, numerical modeling, parameter study

* Corresponding author. Tel.: +852 2766 5816; fax: +852 2765 7198
E-mail address: hong-xing.yang@polyu.edu.hk (H. Yang)

1. Introduction

Indirect evaporative cooler (IEC) is an energy efficient and environmental friendly cooling device which uses water evaporation to produce cooling air. It receives increasingly attention in the field of building energy conservation for its high efficient, good comfort, pollution-free and easy maintenance features [1~5]. The most commonly used plate-type IEC consists of alternative wet and dry channels which are separated by thin plates [6]. In the wet channels, the spraying water drops form a thin water film on the plate surface and consistently evaporates into the main stream of the secondary air. The primary air in the adjacent dry channels is cooled down by the low temperature wall without adding moisture. In normal practice, the outdoor fresh air is used for both primary air and secondary air.

Because the air with lower humidity can provide larger evaporation driving force and cooling capacity, the IEC has been widely adopted in hot and dry regions for directly supplying the cooled primary air [7~9]. Its thermal performances influenced by various operation conditions were investigated [10]. Under such weather conditions, the primary air is only sensibly cooled. The IEC's performances under diverse climate regions were also investigated and proved that its ability to diminish annual cooling degree-days is practically ubiquitous in all territory [11]. However, in hot and humid regions, the supply air temperature of the IEC is limited to the high ambient wet-bulb temperature [12], so the device can't be used independently. Correspondingly, the modeling of IEC with only sensible heat transfer in the primary air channels has been fundamentally investigated.

In general, the modeling methods can be classified into analytical approach and numerical approach. For analytical approach, Maclaine-cross and Banks [13] proposed a linear approximate model of wet surface heat exchangers by analogizing with dry surface heat exchangers. Erens and Dreyer [14] made a comparison among Poppe model, Merkel model and simplified model. Alonso [15] developed a more user-friendly simplified model by introducing an equivalent water temperature. Ren [16] developed an analytical model for IEC with parallel/counter flow configurations considering variable Lewis factor and surface wettability. The modified ε-NTU method is a simplified method for IEC modeling by redefining some parameters and assuming a

linear saturation temperature-enthalpy relation of air [17~19]. Kim developed a practical correlation for IEC based on ε-NTU method [20]. The analysis of the heat and mass transfer process of IEC based on exergy theory was also conducted [21].

For numerical approach, the thermal performances of IEC under a wide variety of inlet air conditions, construction type and flow patterns have been investigated by laying different focuses on the evaporation water loss, water film temperature variation, wall longitudinal heat conduction and variable Lewis factor [22~28]. For experimental research, five kinds of heat and mass exchanging materials were selected for comparative experimental study in IEC systems [29]. A two-stage evaporative cooling system with higher cooling ability was tested and evaluated [30,31]. The performances of IEC and heat exchanger in summer and winter operation were theoretical analysis and measured [32].

In recent years, some novel hybrid evaporative cooling systems were proposed for promoting the 'green cooling technology' to more regions [33~37], of which a hybrid air-conditioning system consisting of an IEC and mechanical cooling came into being for using in hot and humid regions. The IEC, installed before an air handling unit (AHU), is used to pre-cool the incoming fresh air for energy conservation of the air-conditioning system [38]. In this system, the cool and dry exhaust air with much lower wet-bulb temperature from air-conditioned space is used as secondary air for enhancing the cooling effect. However, owing to the high dew point temperature of the fresh air in humid areas, condensation probably occurs, which results in not only sensible cooling but also dehumidification effect. The simultaneous heat and mass transfer process in the primary air channel is much more complicated and will greatly affect the IEC performance.

In respect of research on hybrid evaporative cooling system, an experimental study was conducted to investigate the energy saving potential of IEC as a pre-cooling unit combined with PUA (packaged unit air-condition) in Iran [39]. Numerical analysis was conducted to the IEC combined with a cooling/reheating unit [40]. Financial feasibility of a hybrid-mode operation of a direct evaporative cooler (DEC) with an air conditioning unit was studied [41]. These studies

prove that the energy saving and economic benefit are optimistic and attractive for the hybrid cooling system, but condensation case has not been taken into consideration.

It can be observed that the modeling of IEC with condensation from primary air has seldom been reported by previous studies. Besides, a comprehensive parameter study of IEC under condensation state is also lacking. Therefore, an IEC model considering condensation and a comprehensive parameter study are needed for better predicting the performance and optimization of the hybrid cooling system. The comparison between some representative IEC parameter studies and present study is listed in Table 1.

Table 1 Comparison with other parameter studies

Study	IEC type	Research method	Studied parameters and ranges	Particular study points
[42]	cross flow plate type IEC	FDM numerical simulation	air temperature (25~45℃), secondary air humidity (10~90%), primary air velocity (0.5~4.5m/s), mass flow ratio (0.5~2), wettability (0~1), channel gap (2~10mm)	two-dimensional numerical model was used to firstly investigated 6 parameters
[24]	counter flow plate type RIEC	FDM numerical simulation	air temperature (25~45℃), air humidity (7~26g/kg), air velocity (1.5~6.0m/s), channel gap (1~10mm), channel length (0.1~3m), working to intake air ratio (0.05~0.95)	6 major operating parameters were studied for RIEC system. Wet-bulb and dew-point efficiencies were discussed
[43]	M-cycle cross flow IEC	finite-element method	air temperature (20~40℃), air humidity (10~90%), primary air speed (0.5~4.0m/s), secondary air speed (0.17~1.62m/s), supply-to-total air flow rate (0.1~0.9), channel gap (2~20mm), dimensionless channel length (50~600)	analyses into relation between the wet-bulb effectiveness, system COP and operational parameters were undertaken to M-cycle IEC
[44]	counter flow RIEC with finned channels	experiment & numerical simulation	evaporation water flow rate (0.15 ~ 1.0 lpm), extraction ratio (0.2~0.5), air temperature (27.5~32℃), air humidity (9.19~18.11 g/kg)	counter flow fin-inserted RIEC were experimental tested and numerical simulated; influence of water flow rate were investigated
Present study	counter flow plate type IEC	FDM numerical simulation	primary air temperature (24~40℃), humidity (30~90%), velocity (0.5~5.0m/s); secondary air temperature (20~28℃), humidity (40~70%), velocity (0.5~5.0m/s); wettability (0~1), channel gap (2~10mm), IEC height (0.1~2.0m)	focus on IEC performance with condensation from high humidity primary air using four evaluation indexes

To make up the research gap, a novel numerical model considering condensation from primary air was established. The model was validated by the published data from the literatures. Then, a comprehensive parameter study was conducted with the established numerical model. The effect of nine parameters (including temperature and humidity of primary air and secondary air, channel gap, wettability and cooler height) were analyzed in detail under three operation states (non-condensation, partial condensation and total condensation) by four proposed evaluation indexes(condensation ratio, wet-bulb efficiency, enlargement coefficient and total heat transfer rate). The study results can provide references for evaluation of the hybrid cooling system and optimization of the IEC applied in hot and humid regions.

Nomenclatures

A	heat transfer area, m^2	d_e	hydraulic diameter of channel, m
B	barometric pressure, Pa	h	heat transfer coefficient, $W/m^2 \cdot ℃$
H	cooler height, m	h_m	mass transfer coefficient, $kg/m^2 \cdot s$
L	cooler length, m	h_{fg}	latent heat of vaporization of water, J/kg
P	water vapor pressure, Pa	i	enthalpy of air, J/kg
R	condensation ratio	m	mass flow rate, kg/s
T	thermodynamic temperature, K	n	number of channels
Pr	Prandtl number	q	total heat transfer rate per unit mass, kW/kg
NTU	number of heat transfer unit	s	channel gap, m
c_{pa}	specific heat of air, $J/kg \cdot ℃$	t	Celsius temperature, ℃
c_{pw}	specific heat of water, $J/kg \cdot ℃$	u	air velocity, m/s

Greek symbols

ω	moisture content of air, kg/kg	μ	dynamic viscosity, Pa·s
σ	wettability	υ	kinematic viscosity, m^2/s
η	wet-bulb effectiveness	λ	thermal conductivity, $W/m \cdot ℃$
ε	enlargement coefficient		

Subscripts

c	condensation	cw	condensate water
e	evaporation	ew	evaporation water
p	primary/fresh air	qb	saturation vapor pressure
s	secondary air	wb	wet-bulb temperature
w	wall	sat	saturated humidity

2. Three condensation states of IEC

When an IEC hybrid cooling system is applied in hot and humid regions, the humidity of the primary air is high and the wet-bulb temperature of the secondary air from air-conditioned space is low. So condensation will occur at the place where the plate surface temperature is lower than the dew point temperature of the primary air. According to different inlet air conditions, three possible operation states of IEC can be identified, which are total condensation, partial condensation and non-condensation, as shown in Fig.1. Non-condensation state occurs when the inlet primary air is dry and the dew point temperature is always lower than the plate surface temperature. Total condensation state occurs when the inlet primary air is very humid so that the dew point temperature is higher than the plate surface temperature at the starting point of the inlet air side. In the partial condensation state, the condensation is not taking place until the plate surface temperature is equal to the dew point temperature of the air.

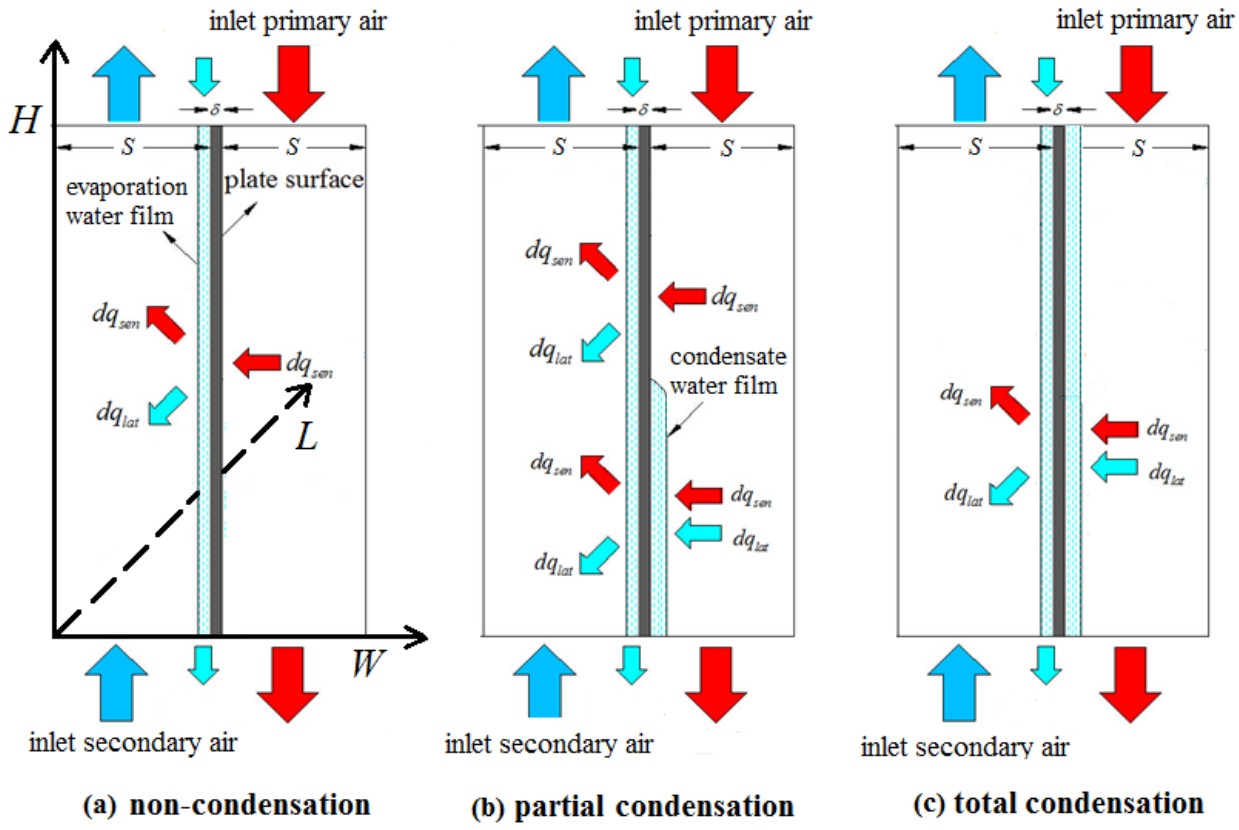

Fig.1 Three condensation states of IEC

3. Modeling of IEC considering condensation

The following part presents a new model of IEC considering the condensation from primary air. The model is based on the following assumptions: 1) Air flows are fully developed and thermal properties of the air and water are constant; 2) The unit is adiabatic, i.e., there is no heat transfer to the surroundings; 3) Both the water film and wall are very thin so the thermal resistances are negligible; 4) Heat and mass are only transferred vertically across the separated plate; 5) The water film is continuously replenished at the same temperature and the condensate water temperature is equal to the dew point temperature of primary air; 6) Lewis number is unity in both evaporation and condensation surface.

The heat balance of the secondary air is calculated as:

$$h_s(t_w - t_s)dA = c_{pa} m_s dt_s \quad (1)$$

The mass balance of the secondary air is calculated as:

$$h_{ms}(\omega_{t_w} - \omega_s)d(\sigma A) = m_s d\omega_s \quad (2)$$

If the local plate surface temperature is higher than dew point temperature of primary air, i.e., $t_w > t_{dew,p}$, only sensible heat exchange will take place in the primary air channels. The heat balance equation of the primary air, mass balance of evaporation water film and energy balance equation of the control volume are calculated as Equation (3) to (5), respectively.

$$h_p(t_p - t_w)dA = c_{pa} m_p dt_p \quad (3)$$

$$dm_e = m_s d\omega_s \quad (4)$$

$$m_s di_s - c_{pa} m_p dt_p = d(c_{pw} t_{ew} m_e) \quad (5)$$

If the local plate surface temperature is lower than dew point temperature of primary air, i.e., $t_w < t_{dew,p}$, the condensation will take place and the moisture is released from the primary air to the plate surface. The heat and mass balance equation of the primary air, mass balance of evaporation water film and condensate water film, as well as the energy balance equation of the control volume are calculated as Equation (6) to (10), respectively.

$$h_p(t_p - t_w)dA = c_{pa} m_p dt_p \quad (6)$$

$$h_{mp}(\omega_p - \omega_{t_w})dA = m_p d\omega_p \quad (7)$$

$$dm_e = m_s d\omega_s \quad (8)$$

$$dm_c = -m_p d\omega_p \quad (9)$$

$$m_s di_s - m_p di_p = d(c_{pw} t_{ew} m_e) + d(c_{pw} t_{cw} m_c) \quad (10)$$

In sum, the Equation (1) ~ (5) form the enclosed governing equations of IEC without considering condensation from primary air; while the Equation (1) ~ (2) and Equation (6) ~ (10) form the enclosed governing equations of IEC with condensation from primary air. In the model, the moisture content of saturated air at plate surface temperature was simplified as a linear function of plate surface temperature, i.e., $\omega_{t_w} = at_w + b$ (kg/ kg). By fitting the exact solutions of moisture content of saturated air as Equation (11) and (12), the constants *a* and *b* in the above simplified linear function were set as 0.0012 and -0.0107, respectively, for the temperature range of 20℃ to 30℃.

$$In\left(P_{qb}\right) = \frac{a_1}{T_w} + a_2 + a_3 T_w + a_4 T_w^{\ 2} + a_5 T_w^{\ 3} + a_6 In\left(T_w\right) \quad (11)$$

$$\omega_{t_w} = 0.622 \frac{P_{qb}}{B - P_{qb}} \quad (12)$$

where,

$a_1 = -5800.2206, a_2 = 1.3914993, a_3 = -0.048640239, a_4 = 0.41764768 \times 10^{-4}, a_5 = -0.14452093 \times 10^{-7}$, $a_6 = 6.5459673$

In the governing equations of IEC without condensation, we substitute Equation (1) ~ (4) into Equation (5) by adopting the enthalpy calculation equation for moisture air $i = c_p t + h_{fg}\omega$, and then re-arrange the equation, the plate surface temperature under non-condensation state can be obtained:

$$t_w = c_1 t_p + c_2 \omega_s + c_3 t_s + c_4 \quad (13)$$

Where,

$$c_1 = \frac{h_p}{h_s + h_p + \sigma a h_{ms}(h_{fg} - c_{pw} t_{ew})}, c_2 = \frac{(h_{fg} - c_{pw} t_{ew}) h_{ms} \sigma}{h_s + h_p + \sigma a h_{ms}(h_{fg} - c_{pw} t_{ew})}$$

$$c_3 = \frac{h_s}{h_s + h_p + \sigma a h_{ms}(h_{fg} - c_{pw} t_{ew})}, \ c_4 = \frac{(c_{pw} t_{ew} - h_{fg}) h_{ms} b \sigma}{h_s + h_p + \sigma a h_{ms}(h_{fg} - c_{pw} t_{ew})}$$

In the governing equations of IEC with condensation, we substitute Equation (1) ~ (2) and (6) ~ (9) into Equation (10) and re-arrange the equation, the plate surface temperature under condensation state can be obtained:

$$t_w = c_5 t_p + c_6 \omega_p + c_7 t_s + c_8 \omega_s + c_9 \qquad (14)$$

where,

$c = h_s + h_p + a h_{fg}(\sigma h_{ms} + h_{mp}) - a c_{pw}(t_{ew}\sigma h_{ms} + t_{cw} h_{mp})$, $c_5 = \frac{h_p}{c}$, $c_6 = \frac{h_{fg} h_{mp} - c_{pw} t_{cw} h_{mp}}{c}$, $c_7 = \frac{h_s}{c}$,

$c_8 = \frac{\sigma h_{fg} h_{ms} - \sigma c_{pw} t_{ew} h_{ms}}{c}$, $c_9 = \frac{b c_{pw}(t_{ew} h_{ms}\sigma + t_{cw} h_{mp}) - b h_{fg}(h_{ms}\sigma + h_{mp})}{c}$.

The heat and mass transfer coefficients were estimated as follows. As the channel gap of the IEC is very small and the air velocity is usually less than 5m/s for ensuring efficient heat transfer, the air flow can be regarded as laminar flow in the IEC device. The distance required for the laminar fully developed flow can be estimated by L/d_e=0.05*(Re*Pr) [45]. In usual application, the typical air velocity is about 2m/s and channel gap is no more than 5mm. So the calculated thermal entry length for fully developed flow is 0.4m, which is smaller than the commonly used IEC in the market. As a result, the thermal effect can be regarded as fully developed. The equation for calculating the heat transfer coefficient for the fully developed laminar flow in the parallel primary air channel and secondary air channel are:

$$h_p = \frac{0.023\left(\frac{u_p}{\upsilon_p}\right)^{0.8} \cdot Pr_p^{0.3} \cdot \lambda_p}{d_e^{\,0.2}} \qquad (15)$$

$$h_s = \frac{0.023\left(\frac{u_s}{\upsilon_s}\right)^{0.8} \cdot Pr_s^{0.3} \cdot \lambda_s}{d_e^{\,0.2}} \qquad (16)$$

The mass transfer coefficient (h_{mp}, h_{ms}) can be obtained accordingly by adopting the analogy law betweenheat and mass transfer, i.e., the Lewis relationship is satisfied and regarded as unity in air-water interaction surfaces [46~48]. So the mass transfer coefficients are:

$$h_{mp} = \frac{h_p}{c_p Le_p^{2/3}} \approx \frac{h_p}{c_p} \quad (17)$$

$$h_{ms} = \frac{h_s}{c_p Le_s^{2/3}} \approx \frac{h_s}{c_p} \quad (18)$$

Different types of number of heat transfer units (NTU) and dimensionless height (x^*) of IEC can be defined as follows:

$$NTU_p = \frac{h_p A}{m_p c_{pa}},\ NTU_{mp} = \frac{h_{mp} A}{m_p},\ NTU_s = \frac{h_s A}{m_s c_{pa}},\ NTU_{ms} = \frac{h_{ms} A}{m_s},\ NTU_e = Ah_{ms},\ NTU_c = Ah_{mp},$$

$$x^* = \frac{x}{H}$$

The above governing equations can be re-written in standard ordinary differential equations as Equation (19) to (24). Then, the differential term is discretized into algebraic form by finite difference method (FDM) and numerical simulation results at each discrete node can be obtained by solving a set of algebraic equations simultaneously. The corresponding wall temperature under non-condensation state and condensation state at each discrete node can be calculated by Equation (13) and Equation (14), respectively.

$$\frac{dt_s}{dx^*} = NTU_s(t_w - t_s) \quad (19)$$

$$\frac{d\omega_s}{dx^*} = \sigma NTU_{ms}(\omega_{t_w} - \omega_s) \quad (20)$$

$$\frac{dt_p}{dx^*} = NTU_p(t_p - t_w) \quad (21)$$

$$\frac{d\omega_p}{dx^*} = NTU_{mp}(\omega_p - \omega_{t_w}) \text{ (if } \omega_p > \omega_{t_w}) \quad (22)$$

$$\frac{dm_e}{dx^*} = \sigma NTU_e(\omega_{t_w} - \omega_s) \quad (23)$$

$$\frac{dm_c}{dx^*} = -NTU_c(\omega_p - \omega_{t_w}) \text{ (if } \omega_p > \omega_{t_w}) \quad (24)$$

The boundary conditions for the above governing equations are:

$$\begin{cases} x^* = 1, t_p = t_{p,in} \\ x^* = 1, \omega_p = \omega_{p,in} \\ x^* = 0, t_s = t_{s,in} \\ x^* = 0, \omega_s = \omega_{s,in} \\ x^* = 1, m_c = 0 \\ x^* = 1, m_e = m_{e,in} \end{cases}$$

The simulation flow chart for solving the governing equations is shown as Fig.2.

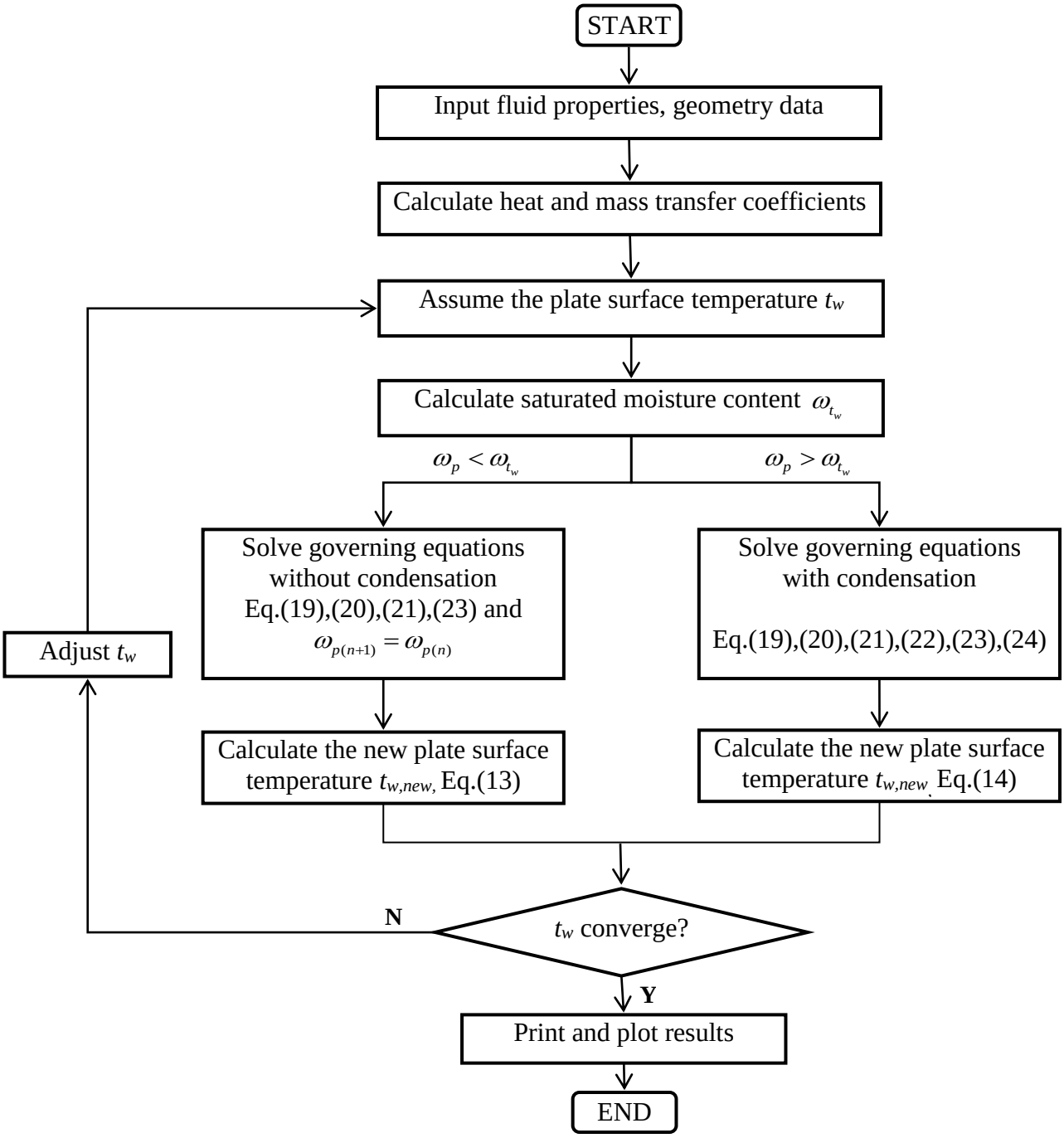

Fig.2 Simulation flow chart for solving the IEC model

To solve the one-dimensional governing equations numerically, the height of the IEC was divided into a series of continuous elements. The grid independency of the developed model has been checked with different mesh sizes from 10 to 250. The optimal number of domain elements was determined by increasing elements until the outlet primary air temperature and moisture

content remains steady. As shown in Fig.3, 100 elements were selected as a compromise between the calculation accuracy and time expense.

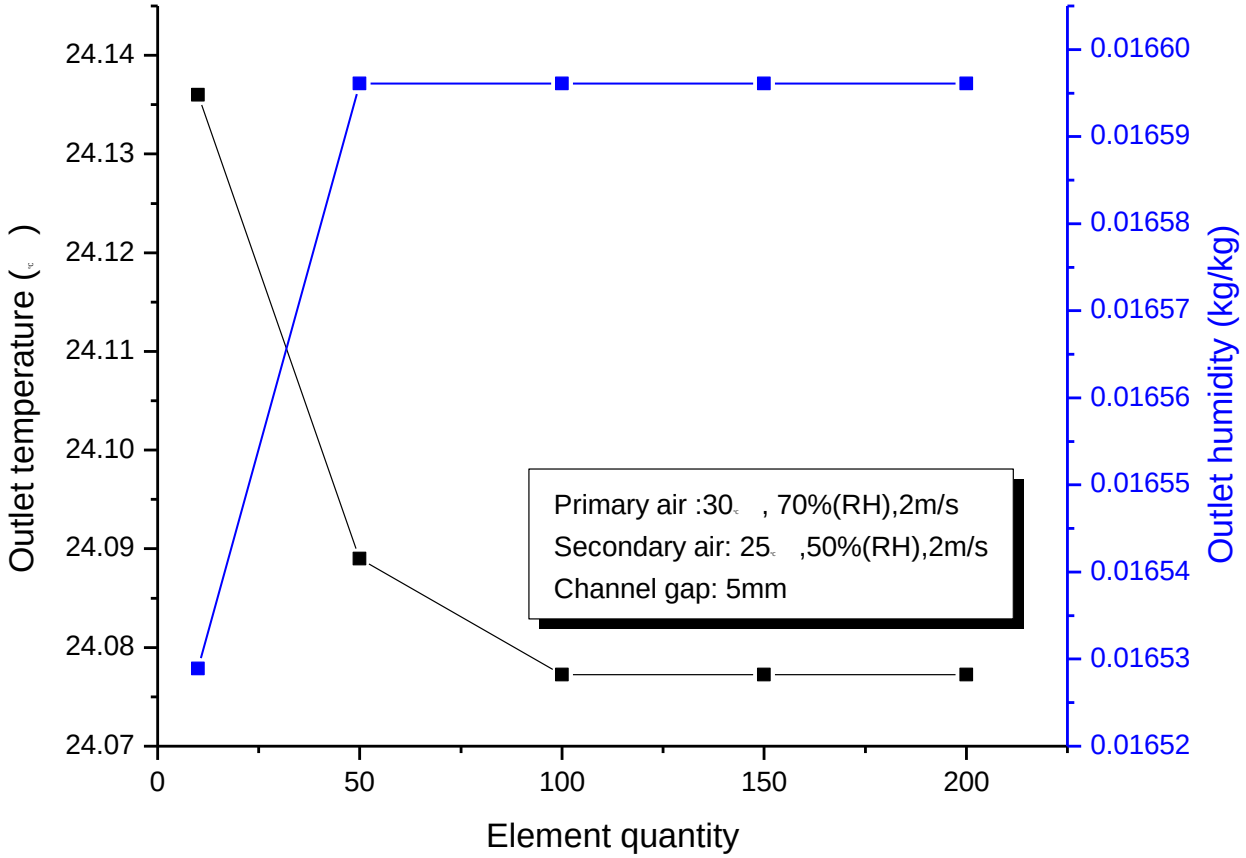

Fig.3 Outlet parameters under different element quantity

The wet-bulb effectiveness is usually used as an evaluation metric for rating an IEC. It is a parameter describing the extent of the approach of the outlet primary air temperature against the wet-bulb temperature of the inlet secondary air, and expressed as [49]:

$$\eta_{wb} = \frac{t_{p,in} - t_{p,out}}{t_{p,in} - t_{wb,s}} \tag{25}$$

The wet-bulb effectiveness can only describe the ability of IEC in handling sensible heat. However, under the condensation condition, other evaluation indexes are needed for evaluating the IEC ability in handling latent heat. Therefore, three other indexes were introduced for comprehensively evaluating the IEC performance, including condensation ratio R_{con}, enlargement coefficient β and total heat transfer rate q_{tot}.

The condensation ratio R_{con} is defined as the proportion of condensation area to the total heat exchanger area as Equation (26). The condensation ratio is 0 when there is no condensation from primary air and it is 1 when condensation takes place at the entire separated wall. The condensation ratio varies from 0 to 1 under partial condensation.

$$R_{con} = \frac{A_{con}}{A} \tag{26}$$

The enlargement coefficient ε is introduced for evaluating the enlarged heat transfer rate associated with condensation. As shown in Equation (27), it is calculated as the total heat transfer rate divided by the sensible heat transfer rate. Under the non-condensation state, the enlargement coefficient equals 1.

$$\varepsilon = \frac{Q_{tot}}{Q_{sen}} = \frac{c_{pa} \cdot m_p \cdot (t_{p,in} - t_{p,out}) + h_{fg} \cdot m_p \cdot (\omega_{p,in} - \omega_{p,out})}{c_{pa} \cdot m_p \cdot (t_{p,in} - t_{p,out})} \tag{27}$$

The total heat transfer rate per unit mass q (kW/kg) is an index for evaluating the total heat removed from primary air or its enthalpy drop per unit mass, expressed as:

$$q = \frac{Q_{tot}}{M_p} = \frac{c_{pa} \cdot m_p \cdot (t_{p,in} - t_{p,out}) + h_{fg} \cdot m_p \cdot (\omega_{p,in} - \omega_{p,out})}{m_p \cdot (\frac{H}{u_p})} \tag{28}$$

4. Model comparison

The newly developed IEC model was compared with the other study results derived from published papers for two different operation states: IEC without condensation from primary air and IEC with condensation from primary air. Firstly, the numerical simulation results of a dew point IEC derived by B. Riangvilaikul [24] were employed to compare the temperature distribution of the primary air and humidity distribution of the secondary air of the IEC without condensation. In this kind of IEC, a certain fraction of the outlet primary air is diverted into the wet channel to act as the secondary air. The simulations were conducted with the present developed model by setting the same flow pattern, unit geometry and inlet air conditions as given in the literature. Two representative cases with high humidity (35℃, 21.1g/kg) and low humidity (35℃, 8.5g/kg) of inlet air were both compared. The comparisons of the simulation results

between the two models are presented in Fig.4. It was found that the newly developed numerical model predicts the IEC performance with the discrepancy of 2.8% to 6.3% for outlet primary air and 1.7% to 5.0% for outlet secondary air humidity.

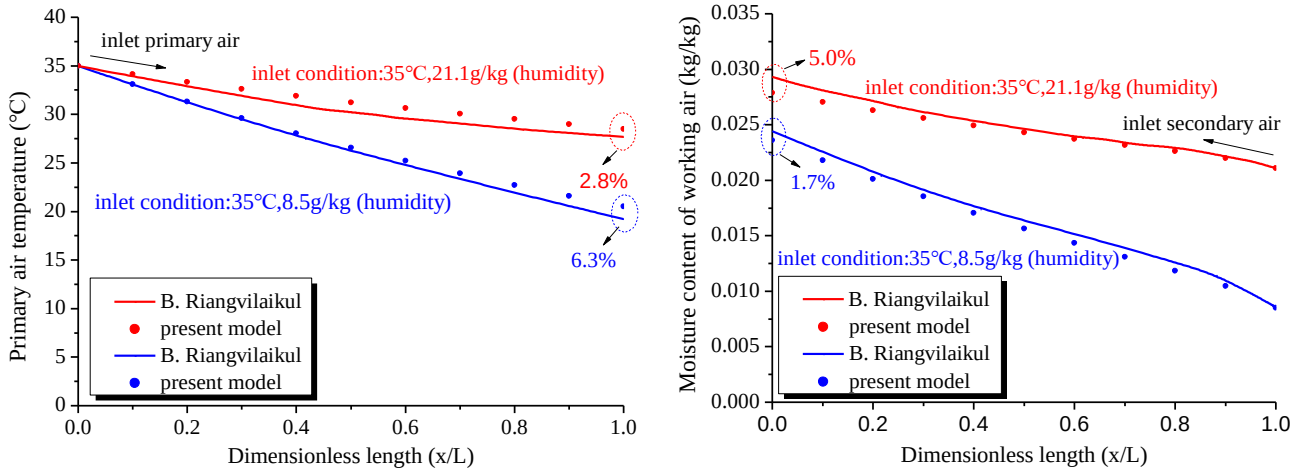

Fig.4 Comparison of simulation results with published data (IEC without condensation)

Next, the simulation results of present model under condensation state were compared with the simulation results in a recently published paper [50]. In this paper, the exhausted air from a conditioned room with the temperature of 25℃ and relative humidity of 50% was used as the secondary air to pre-cool the humid fresh air. The temperature of the inlet fresh air ranges from 30℃ to 37.5℃ while the relative humidity (RH) ranges from 70% to 90%. The condensation from primary air takes place in all the simulation cases, so the primary air moisture content is reduced as well as the temperature. The comparisons between the simulation results of outlet primary air temperature and humidity are shown in Fig.5. It was found that the present numerical model can predict the outlet primary air temperature and humidity with the discrepancy of 5.9% and 2.4%, respectively. Act as a cooling device, the percentage difference of the sensible, latent and total heat transfer rate on primary air side was used as another discrepancy index between the two models, which can be defined as $\varepsilon_{sen}=\left|\frac{q_{sen,pre}-q_{sen,lit}}{q_{sen,lit}}\right|=\left|\frac{t_{out,lit}-t_{out,pre}}{t_{in,lit}-t_{out,lit}}\right|$, $\varepsilon_{lat}=\left|\frac{q_{lat,pre}-q_{lat,lit}}{q_{lat,lit}}\right|=\left|\frac{\omega_{out,lit}-\omega_{out,pre}}{\omega_{in,lit}-\omega_{out,lit}}\right|$ and $\varepsilon_{ent}=\left|\frac{c_p\cdot(t_{out,lit}-t_{out,pre})+h_{fg}\cdot(\omega_{out,lit}-\omega_{out,pre})}{c_p\cdot(t_{in,lit}-t_{out,lit})+h_{fg}\cdot(\omega_{in,lit}-\omega_{out,lit})}\right|$. A discrepancy of 17.0% can be found in predicting the primary air sensible heat transfer rate

between the present numerical model and reference's model; while the discrepancy for latent heat transfer rate was calculated to be 7.9% and total heat transfer rate was 10.9%. The discrepancy can be attributed to the different heat and mass transfer theory adopted in the two models, in which convection mass transfer model and heat and mass analogy theory was used for present model, while Fick's penetration theory was used in literature's model.

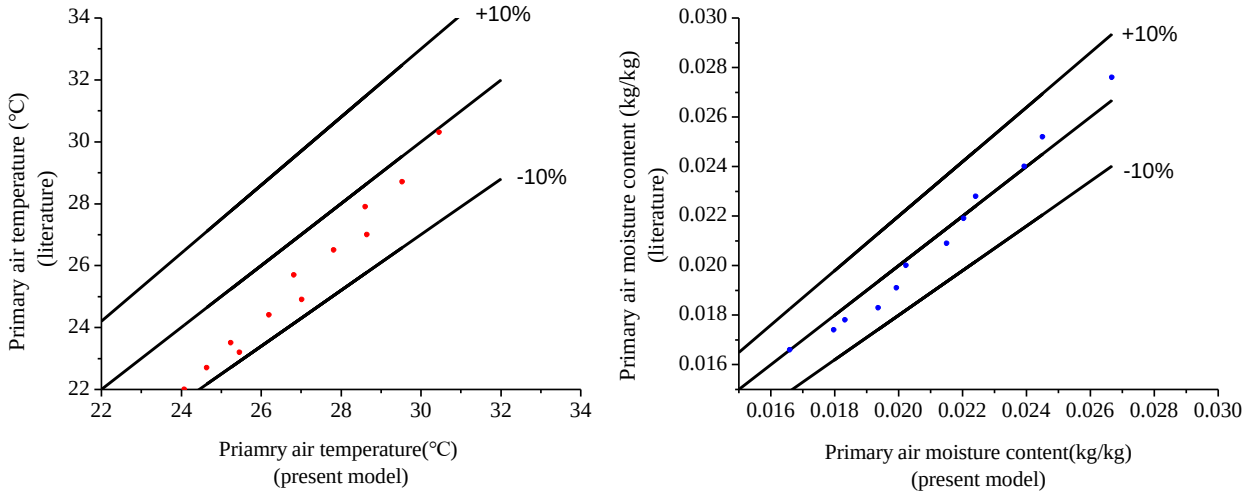

Fig.5 Comparison of simulation results with published data (IEC with condensation)

Based upon the favorable comparison of the two models under both non-condensation and condensation cases, the newly developed IEC model can be used for the following parameter analysis.

5. Results and discussion

5.1 Temperature and humidity distribution

The air temperature and humidity distribution of the IEC with condensation are shown in Fig.6 and Fig.7. Fig.6 presents the IEC performance with partial condensation for the case of t_p =34℃ and RH_p =50% and Fig.7 presents the performance under total condensation for the case of t_p =34℃ and RH_p =70%.

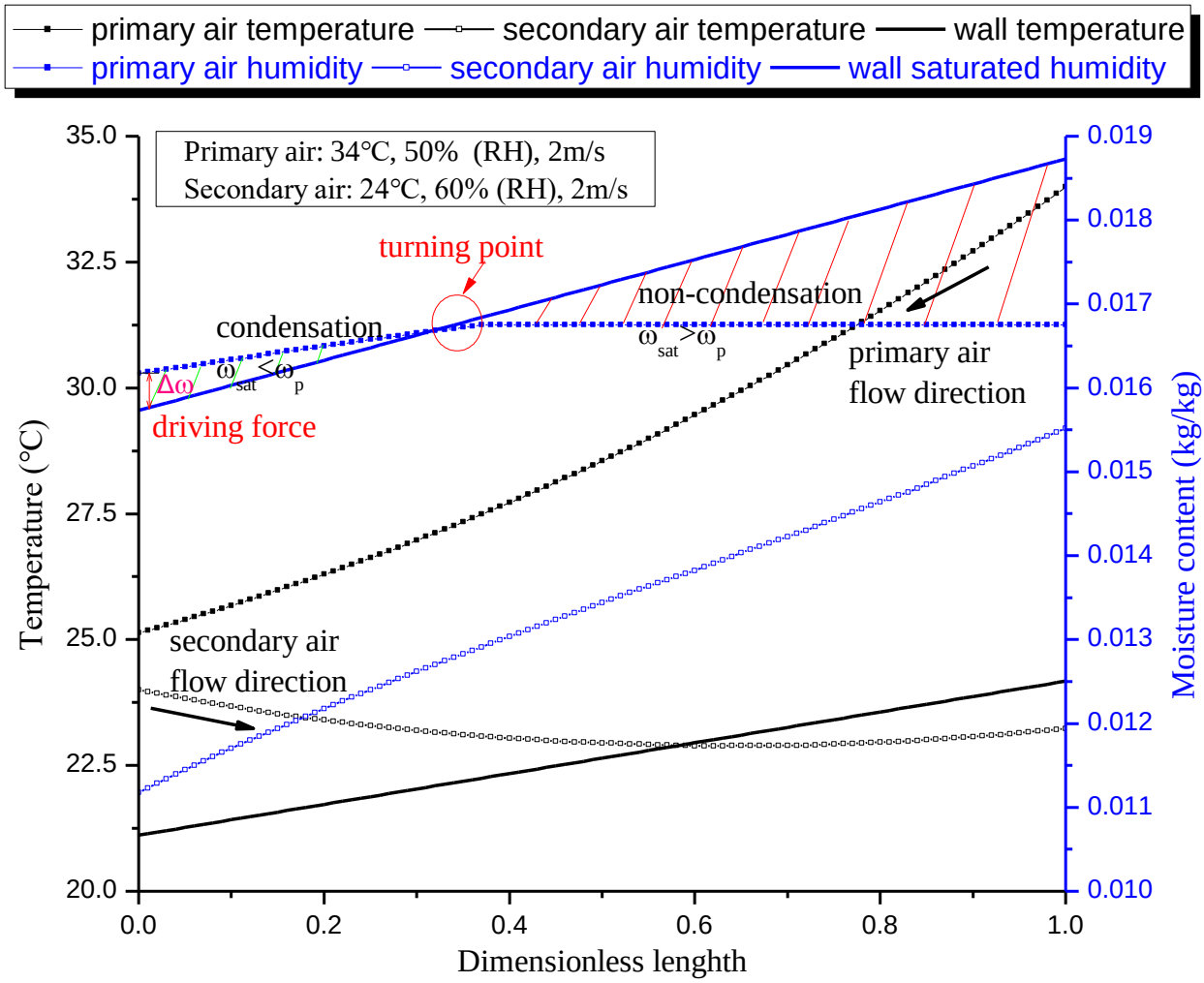

Fig.6 Temperature and humidity distribution of partial condensation

As shown in Fig.6, the primary air temperature keeps decreasing along the flow direction. The humidity remains unchanged at the beginning until it reaches the turning point where it begins to decline constantly. The turning point separates the condensation and non-condensation regions of the primary air channel. In the non-condensation region, $\omega_{sat} > \omega_p$ while in the condensation region, $\omega_{sat} < \omega_p$. At the turning point, the saturated humidity at the wall temperature is equal to the humidity of inlet primary air, in other words, the wall temperature is equal to the dew-point temperature of inlet primary air.

The reason why condensation takes place can be attributed to the humidity of the primary air is higher than the saturated humidity at the local wall temperature. So the excessive moisture of the

primary air is condensed, releasing heat to the surroundings at the same time. The higher the primary air humidity and the lower the wall temperature, the larger the driving force of mass transfer is and the more latent heat is released. In Fig.6, the diving force keeps increasing along the primary air flow direction in the condensation region because the wall temperature is reduced in the same direction.

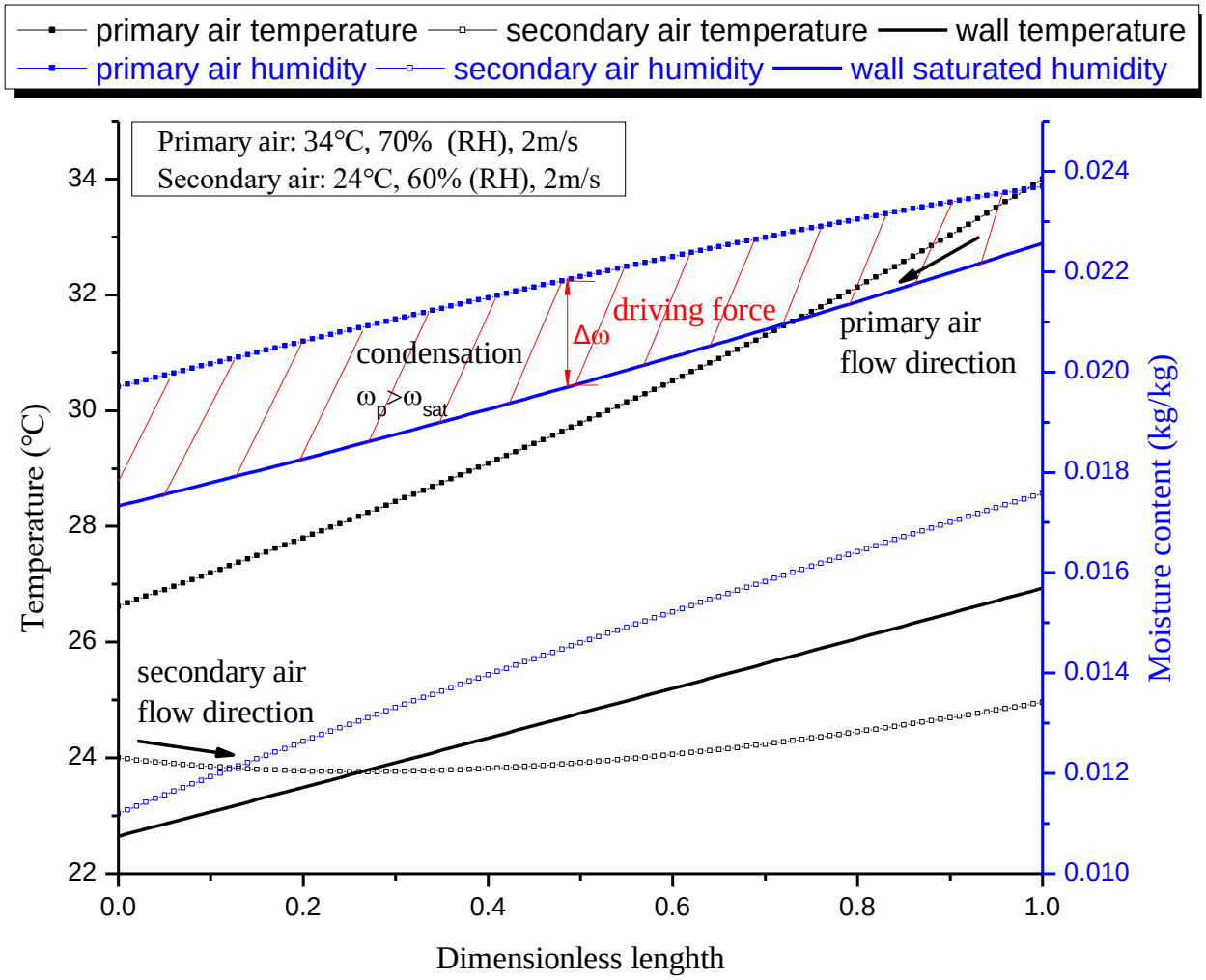

Fig.7 Temperature and humidity distribution of totally condensation

In Fig.7, the primary air humidity keeps decreasing along the flow direction and no turning point exists. Because the high humidity of inlet primary air is higher than the saturated humidity at the entrance, the condensation takes place in the whole channel. It can be seen that the humidity difference is increasing along the primary air flow direction at the beginning and remains relatively constant thereafter. The higher inlet air humidity results in a larger condensation area,

greater mass transfer rate and a higher wall temperature. The average wall temperature in Fig.7 is 24.8℃, 2.2℃ higher than that of Fig.6 because of more heat released by the condensation.

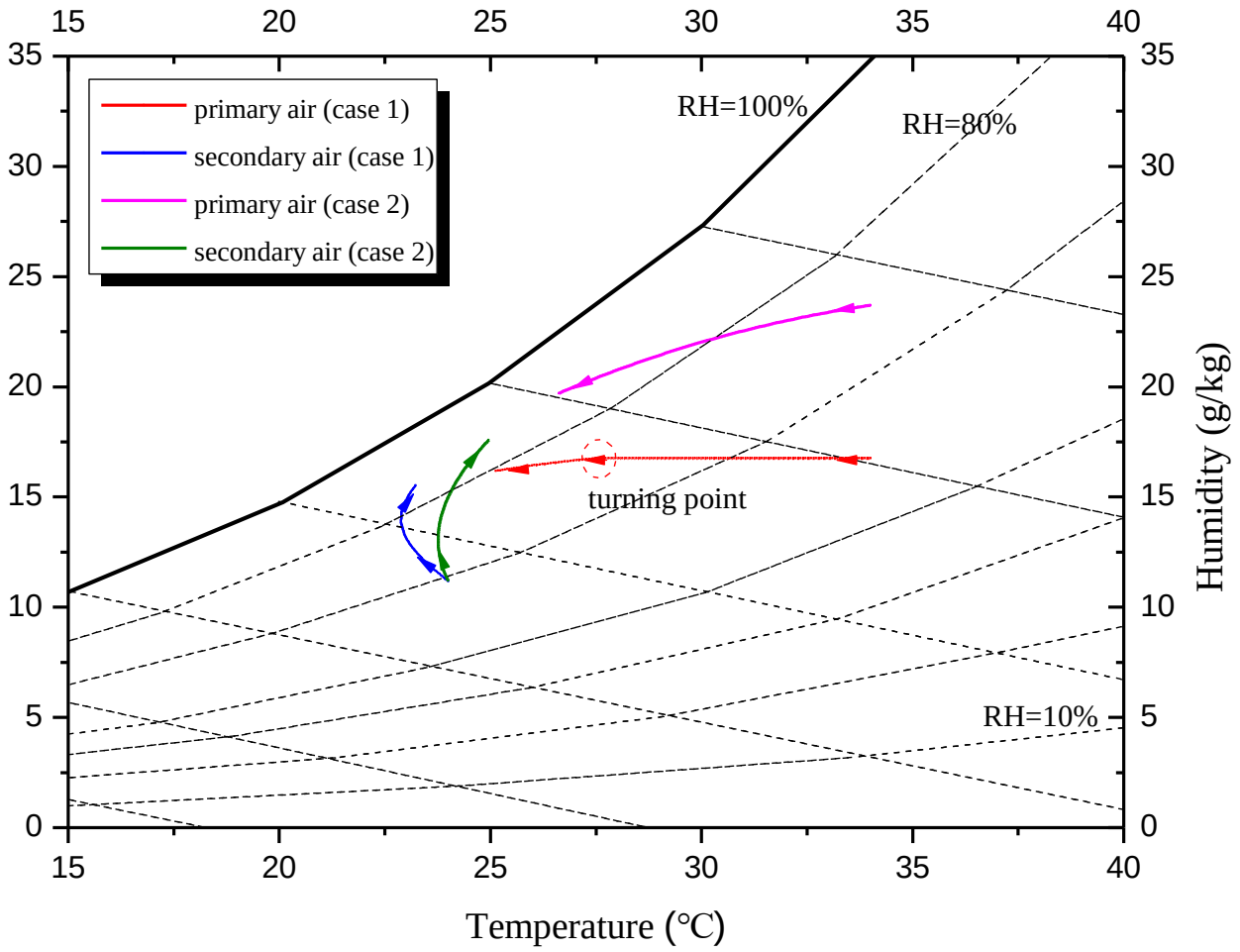

Fig.8 Primary air and secondary air handling process under condensation state

Fig.8 shows the air handling process of the above two cases in the psychrometric chart. It can be seen that the primary air with lower inlet humidity can achieve a lower outlet temperature, so the sensible heat transfer rate is larger. It can be attributed to a lower wall temperature. On the other hand, owing to the higher humidity inlet air, the latent heat transfer rate is enlarged and the outlet air humidity is reduced significantly owing to the stronger condensation effect. It provides a practical application field for IEC dehumidification and pre-cooling in the air-conditioning system. The IEC, acting as a heat recovery device, can counteract part of sensible and latent cooling load of the fresh air, and reduce the energy consumption of the chiller. Comparing the air handling processes of the secondary air in the two cases, the outlet temperature, humidity and

enthalpy under total condensation is significantly larger than that of partial condensation. The reason is that the stronger the condensation effect, the higher the wall temperature is and the larger the sensible heat transfer is between the secondary air flow and wall. The larger outlet humidity is because the saturated air humidity is larger at higher wall temperature, so the water evaporation is therefore enhanced.

Considering the enthalpy change of the primary air, it can be seen that under partial condensation state, the enthalpy drop was calculated to be 10.35 kJ/kg of which the sensible part accounts for 86.1%. While for total condensation, the enthalpy drop was 17.40 kJ/kg, 0.7 times larger than that of partial condensation, but the sensible part only occupies 42.6%. It shows that the condensation can greatly increase the total heat transfer of primary air by enhancing the latent heat transfer, but decreasing the sensible heat transfer.

5.2 Parameter analysis

In this paper, nine influential parameters of IEC were investigated by the newly developed numerical model, including temperature of primary air (t_p), relative humidity of primary air (RH_p), velocity of primary air (u_p), temperature of secondary air (t_s), relative humidity of secondary air (RH_s), velocity of secondary air (u_s), channel gap (s), wettability (σ) and height of cooler (H). In the hybrid IEC pre-cooling system, the temperature and humidity of the secondary air generally vary within a relatively small range as it is the exhausted air from indoor air-conditioned space. In order to compare the IEC performance under different primary air humidity, three levels of relative humidity (30%, 50% and 70%) were selected for each parameter simulation scheme. The detailed arrangement of parameter study is listed out in Table 2. For each studied parameter, the value varied in a range (marked in bold) and the rest remained unchanged.

Table 2 Summary of the ranges of various parameters

Studied object	Parameter values								
	t_p (℃)	RH_p (%)	u_p (m/s)	t_s (℃)	RH_s (%)	u_s (m/s)	s (mm)	σ -	H (m)
t_p	**24~40**	30,50,70	2.0	24	60	2.0	5	1	0.5
RH_p	35	**30~90**	2.0	24	60	2.0	5	1	0.5
u_p	35	30,50,70	**0.5~5**	24	60	2.0	5	1	0.5
t_s	35	30,50,70	2.0	**20~28**	60	2.0	5	1	0.5
RH_s	35	30,50,70	2.0	24	**40~70**	2.0	5	1	0.5
u_s	35	30,50,70	2.0	24	60	**0.5~5**	5	1	0.5
s	35	30,50,70	2.0	24	60	2.0	**2~10**	1	0.5
σ	35	30,50,70	2.0	24	60	2.0	5	**0~1**	0.5
H	35	30,50,70	2.0	24	60	2.0	5	1	**0.1~2**

Then, the effects of various parameters on the thermal performance of the IEC under three operation states (non-condensation, partial condensation and total condensation) were presented and discussed with four evaluations indexes: condensation ratio, wet-bulb efficiency, enlargement coefficient and total heat transfer rate.

5.2.1 Influence of primary air temperature

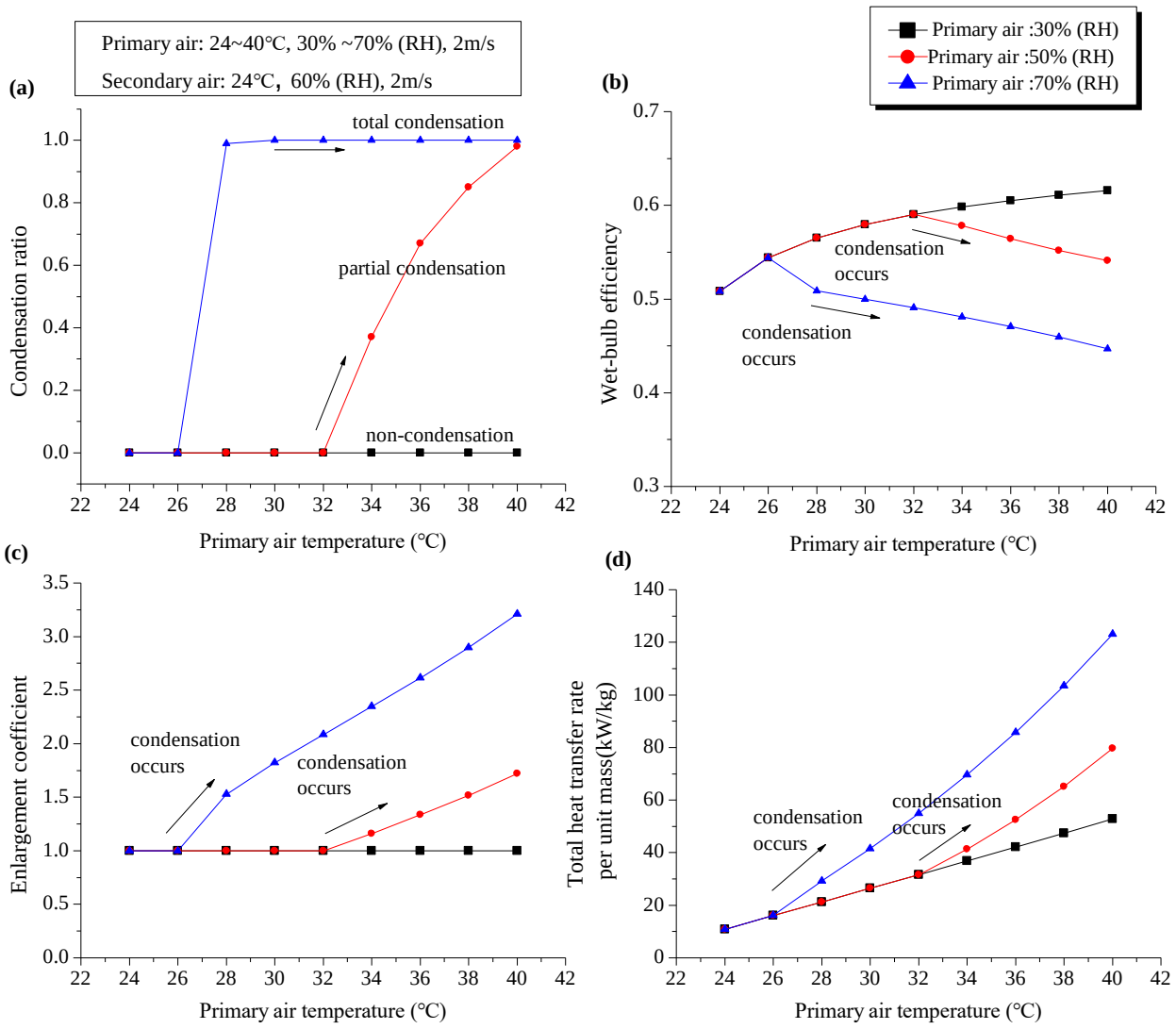

Fig.9 Influence of primary air temperature on: (a) condensation ratio; (b) wet-bulb efficiency; (c) enlargement coefficient; (d) total heat transfer rate per unit mass

Fig.9 presents the influence of primary air temperature on the thermal performance of the IEC. When the air temperature increases with constant relative humidity (RH), the moisture content is increased accordingly. Keeping constant RH_p=50%, the condensation ratio improves significantly from 0 (non-condensation) to 1 (total condensation) when t_p increases from 32℃ to 40℃. Regarding the wet-bulb efficiency, it improves with t_p under the non-condensation state because of the larger temperature difference between the two channels. However, it decreases greatly with the increase of t_p once condensation occurs. The reason is that the heat released

through the condensation process raises the wall temperature and outlet air temperature significantly. The higher the moisture contents of inlet air, the stronger the condensation effect is, and the more significantly the wet-bulb efficiency declines. On the other hand, the enlargement coefficient increases linearly with the increase of t_p under condensation state, which indicates a remarkable boost of latent heat removal of primary air. When t_p=40℃ and RH_p=70%, the latent heat transfer rate accounts for 69% of the total heat transfer rate with the enlargement coefficient of 3.2.

Considering the total heat transfer, it can be seen that under non-condensation state, the total heat transfer rate increased steadily and linearly from 10.9 kW/kg to 52.8 kW/kg when t_p increases from 24℃ to 40℃. However, the growth rate of total heat transfer rate starts to speed up at t_p=32℃ when the partial condensation occurs. The rapid growth can be observed from 31.6 kW/kg to 79.6 kW/kg as t_p increases from 32℃ to 40℃. The growth rate was found to be 1 time larger than that of non-condensation state. Moreover, when the condensation effect becomes stronger, such as 70% RH at total condensation state, the total heat transfer rate further improves. It is 55% to 68% larger than that of partial condensation state at RH of 50% under the same primary air temperature. But the growth rate is similar with each other.

5.2.2 Influence of primary air humidity

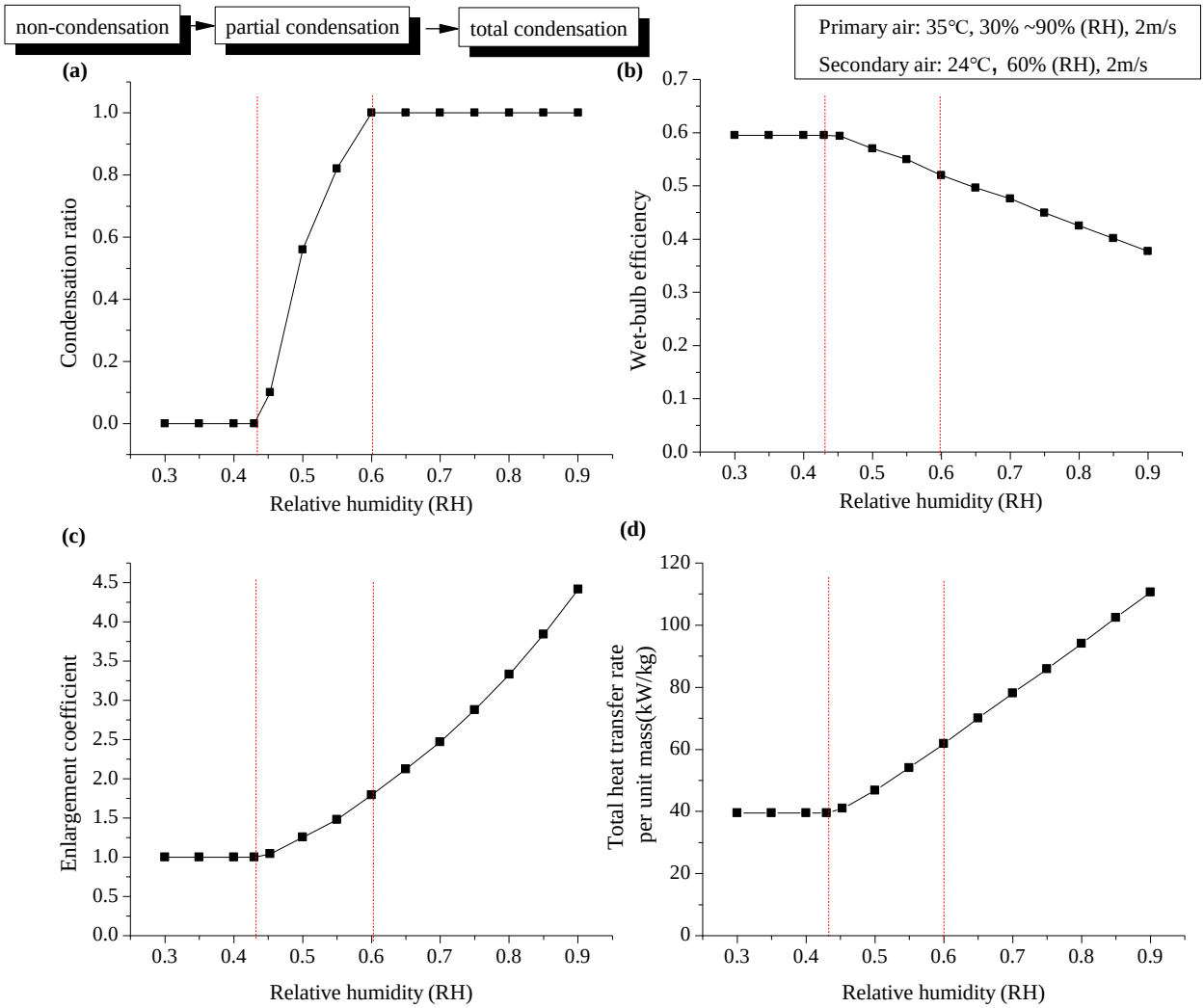

Fig.10 Influence of primary air humidity on: (a) condensation ratio; (b) wet-bulb efficiency; (c) enlargement coefficient; (d) total heat transfer rate per unit mass

Fig.10 presents the influence of primary air RH on the thermal performance of the IEC. With the increase of RH, the condensation ratio shows a growth tendency from 0 to 1, i.e., from non-condensation to partial condensation to total condensation. It improves linearly in the partial condensation region within a relative narrow RH range. Under the non-condensation state, the wet-bulb efficiency, enlargement coefficient and total heat transfer rate do not change with the RH because the sensible heat transfer remains the same. However, the wet-bulb efficiency decreases linearly with the increase of primary air RH under the condensation state as latent heat transfer increases. It drops by 22% as the RH increases from 30% to 90%. The total heat transfer

rate keeps unchanged under non-condensation state. Once the condensation occurs, it increases linearly with the rising of RH no matter under partial or total condensation states. The total heat transfer rate is 1.8 times larger than that of non-condensation state when the RH reaches 90%. The corresponding enlargement coefficient can reach up to 4.5, implying the latent heat transfer accounts for 78% of the total heat transfer.

5.2.3 Influence of primary air velocity

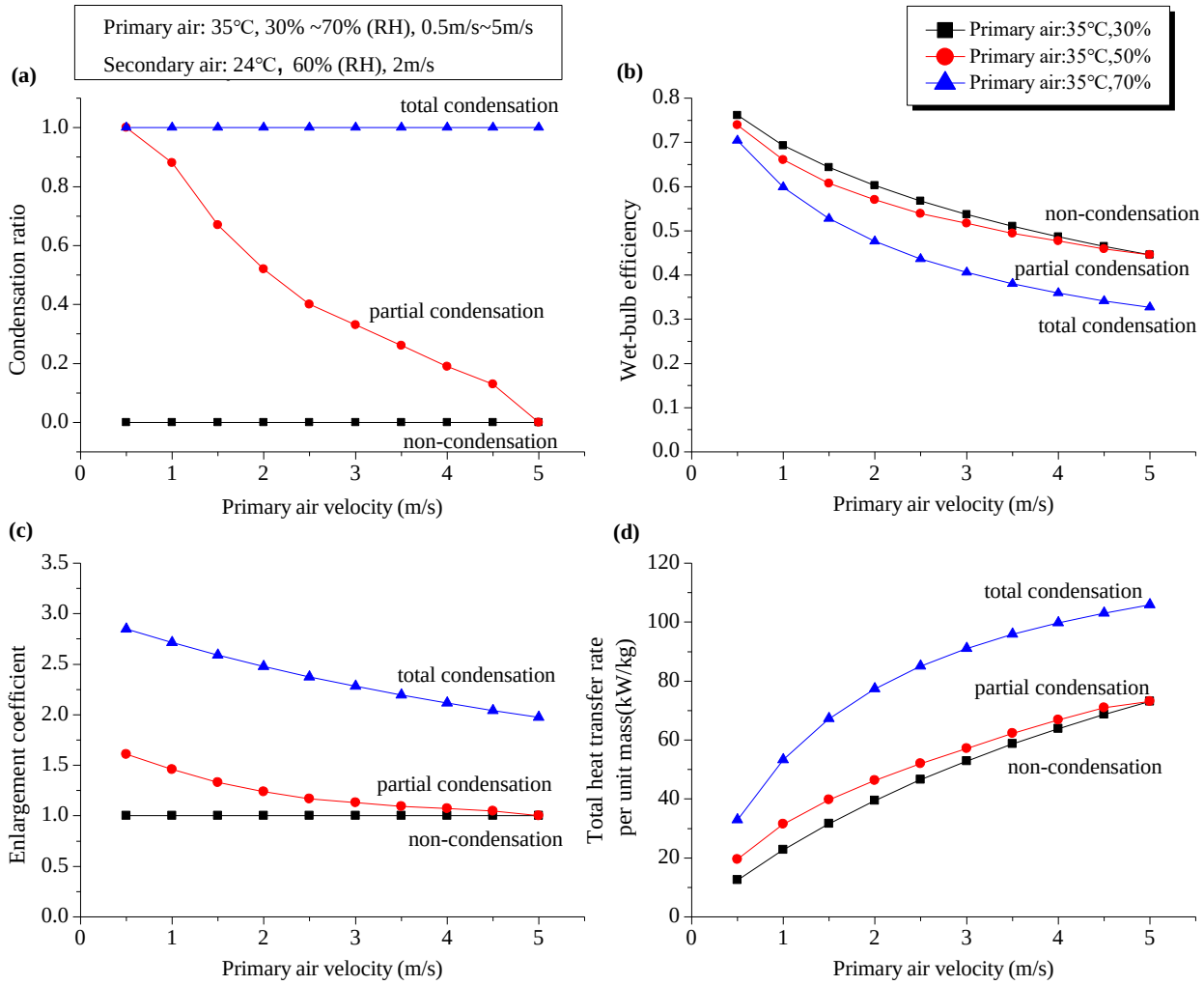

Fig.11 Influence of primary air velocity on: (a) condensation ratio; (b) wet-bulb efficiency; (c) enlargement coefficient; (d) total heat transfer rate per unit mass

Fig.11 presents the influence of primary air velocity on the thermal performance of the IEC. The increase of primary air velocity results in a larger mass flow rate. As the cooling capacity of the

secondary air is constant, the cooling effect is weakened for the primary air. So the condensation ratio declines from 1 (total condensation) to 0 (non-condensation) with the increase of primary air velocity for the case of t_p=35℃, RH_p=50%. Accordingly, the enlargement coefficient also decreases as the cooling demand of primary air increases. As for the wet-bulb efficiency, the curves of three operation states show similar trend, which decrease with the increase of primary air velocity. However, the decline trend for total condensation is more significant than that of the non-condensation state because it involves latent heat transfer process, which has a negative effect on the sensible heat transfer and wet-bulb efficiency. For partial condensation, the trend is more gentle owing to the condensation state's transformation. For the total heat transfer rate, it improves with the increase of primary air velocity mainly because of more cooling carrier provided. But a slower growth rate can be observed under condensation state owing to the weakening of condensation effect.

5.2.4 Influence of secondary air temperature

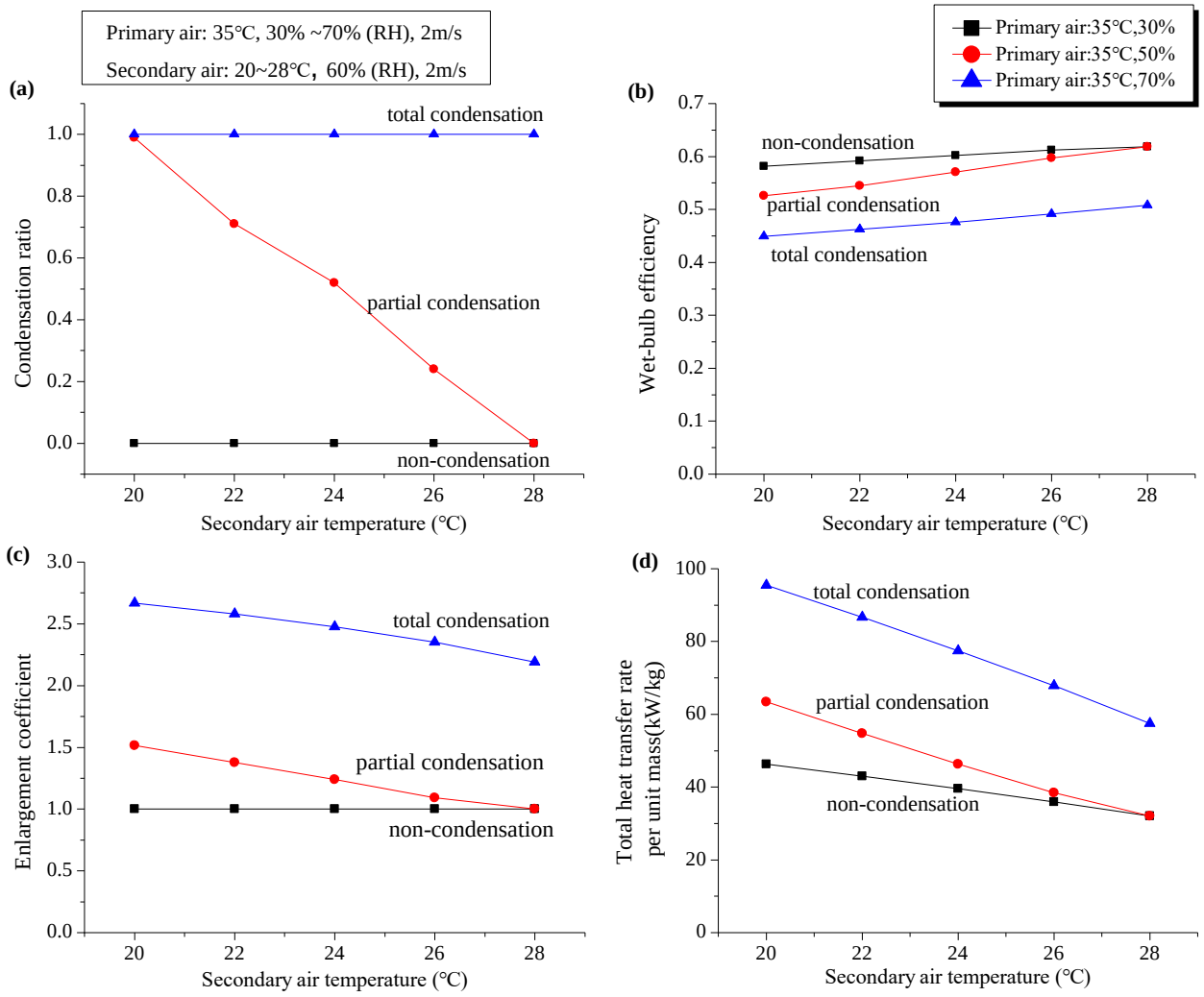

Fig.12 Influence of secondary air temperature on: (a) condensation ratio; (b) wet-bulb efficiency; (c) enlargement coefficient; (d) total heat transfer rate per unit mass

Fig.12 presents the influence of secondary air temperature on the thermal performance of IEC. The wet-bulb temperature of the secondary air, which also indicates the limited outlet temperature of the primary air, will increase with the rising of the dry-bulb temperature at constant RH. The higher the secondary air temperature, the smaller the temperature difference is between the channels, and the less the heat is transferred. So the condensation ratio (at the condition of t_p=35℃, RH=50%), keeps decreasing from total condensation to partial condensation to non-condensation with the secondary air temperature increases from 20℃ to 28℃. Because of the weakened cooling capacity of the secondary air, the enlargement coefficient

also decreases a little for the condensation cases. Besides, the decline trend for the total heat transfer rate can be observed, but the trend is more significant for the condensation state compared with that of non-condensation state. For example, it declines from 46.3 kW/kg to 32.0 kW/kg under non-condensation state (30.9% decrease); from 63.4 kW/kg to 32.0 kW/kg under partial condensation state (49.5% decrease) and from 95.4 kW/kg to 57.5 kW/kg under total condensation state (65.9% decrease). It is owing to the simultaneously decline of the sensible and latent heat transfer.

5.2.5 Influence of secondary air humidity

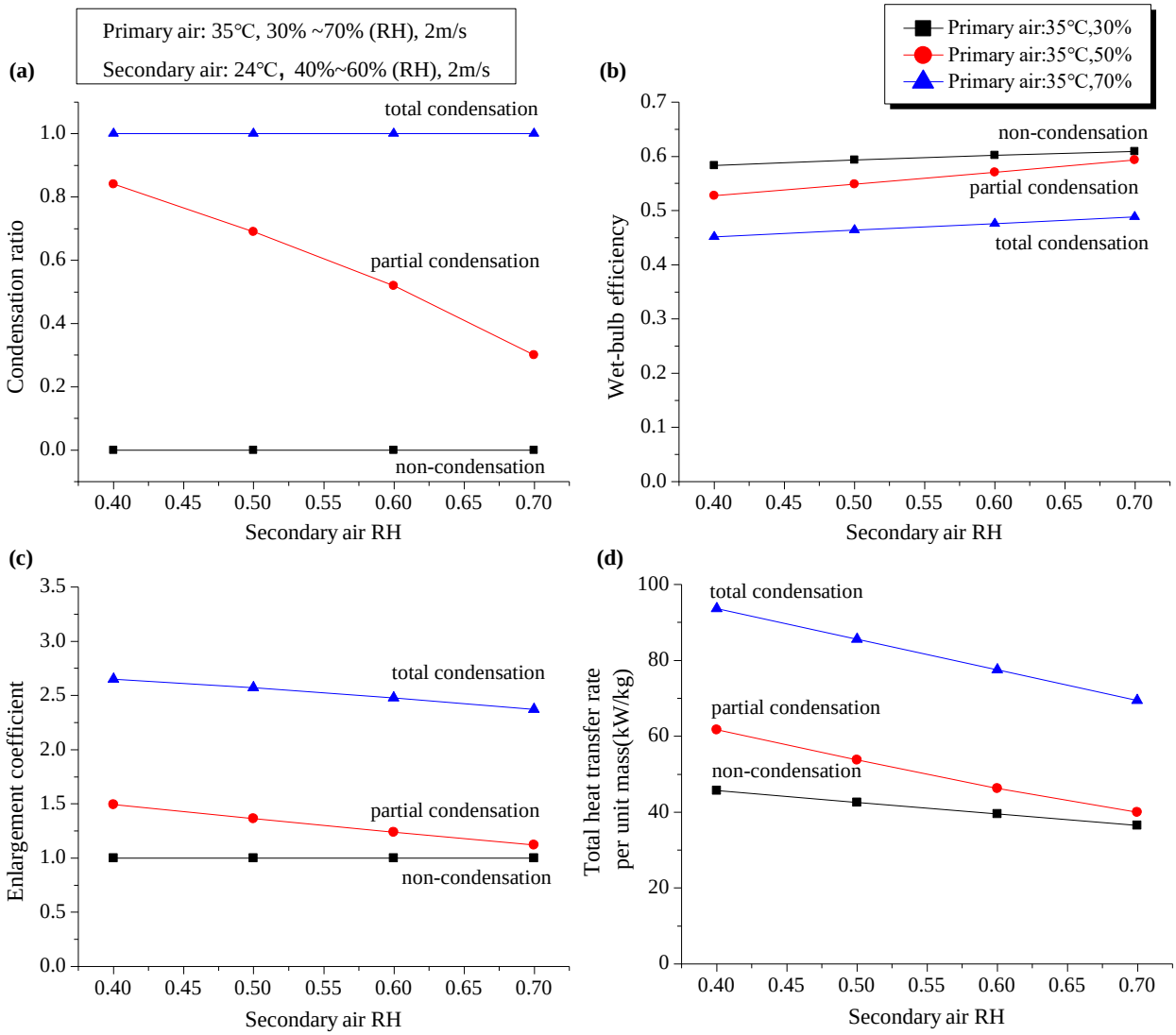

Fig.13 Influence of secondary air humidity on: (a) condensation ratio; (b) wet-bulb efficiency; (c) enlargement coefficient; (d) total heat transfer rate per unit mass

Fig.13 presents the influence of secondary air humidity on the thermal performance of IEC. The wet-bulb temperature of the secondary air increases with the increase of RH. As a result, the higher the RH, the less the cooling capacity could be provided. It will result in the decline of condensation ratio for partial condensation state, decrease of enlargement coefficient for two condensation states and reduction of total heat transfer for all the three operation states. From the point of mass transfer mechanism, the secondary air with lower humidity owns a greater ability to evaporate because of the larger driven force brought by the water vapor concentration difference between the wall surface and mainstream air flow.

5.2.6 Influence of secondary air velocity

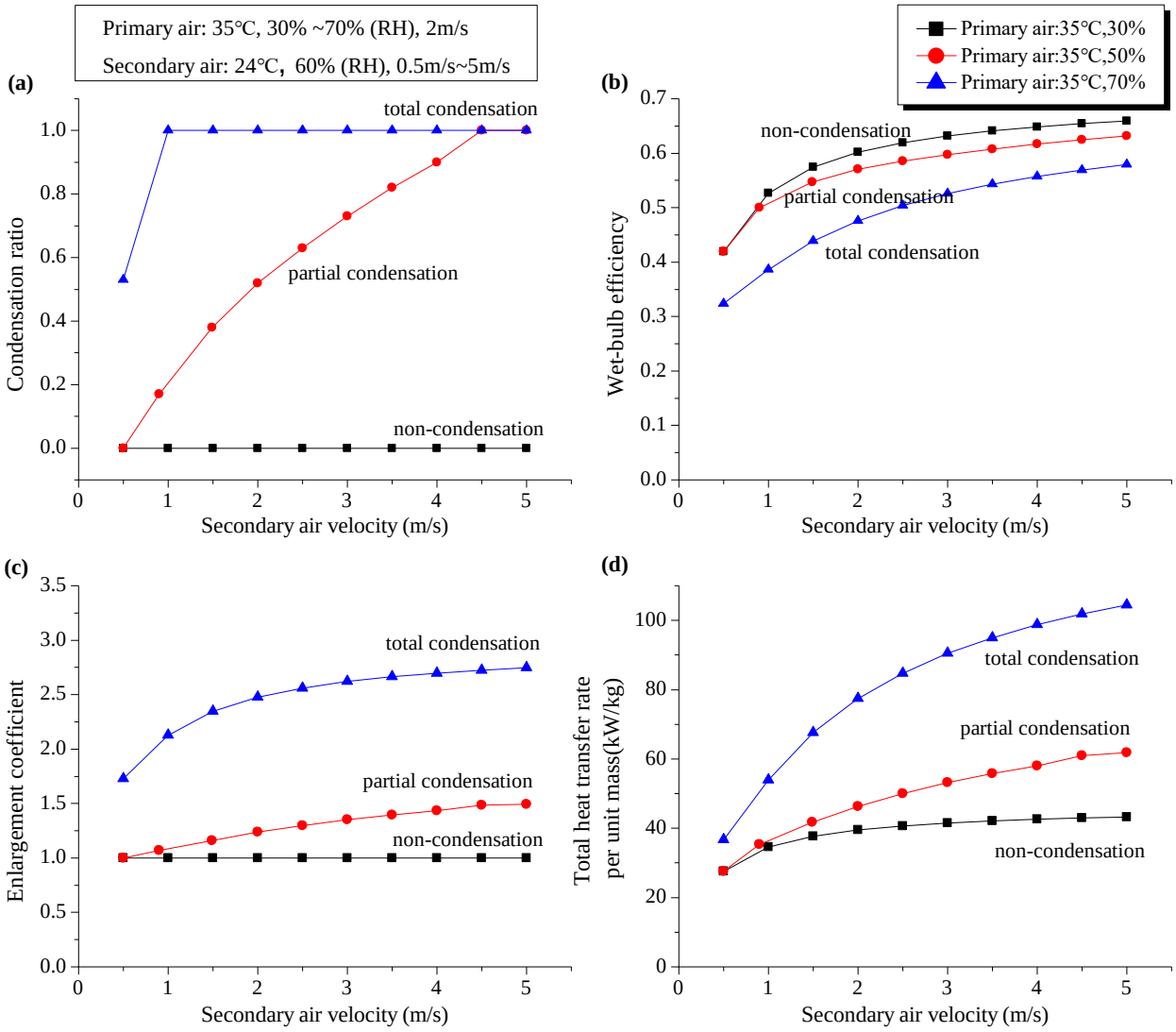

Fig.14 Influence of secondary air velocity on: (a) condensation ratio; (b) wet-bulb efficiency; (c) enlargement coefficient; (d) total heat transfer rate per unit mass

Fig.14 presents the influence of secondary air velocity on the thermal performance of IEC. In contrast with the negative effect brought by the rise of primary air velocity, the increase of secondary air velocity can enhance the cooling effect because of the larger mass flow rate of the cooling media. As shown in Fig.14, the condensation ratio improves from 0 to 1 dramatically as the secondary air velocity increases from 0.5m/s to 5.0m/s. It can be deduced that the wall temperature is greatly reduced with the increase of the mass flow rate of secondary air and brings condensation. The higher velocity of secondary air can result in higher wet-bulb efficiency, larger enlargement coefficient for condensation state and total heat transfer rate.

However, the growth rates of wet-bulb efficiency and total heat transfer rate are different for non-condensation state and the condensation state. For non-condensation state, the growth rate is very significant at the beginning when u_s increases from 0.5m/s to 1.5m/s (the flow rate ratio of secondary air to primary air is about 0.25 to 0.75), then slows down thereafter. When u_s is larger than 3.0m/s (the flow rate ratio of secondary air to primary air exceeds 1.5), the improvement is limited. While for condensation state, the growing rate for wet-bulb efficiency and total heat transfer rate are more obvious even though the flow rate ratio reaches 1.5. It can be explained as: the enhancement effect of adding secondary air flow rate not only improves the sensible heat transfer but also strengthen the latent heat transfer. Thus, the increase of secondary air velocity can be a more effective measure for enhancing the cooling effect of IEC under condensation state. But it also needs to pay attention that the secondary air velocity should not be too large because it might result in insufficient mass transfer with water film.

5.2.7 Influence of channel gap

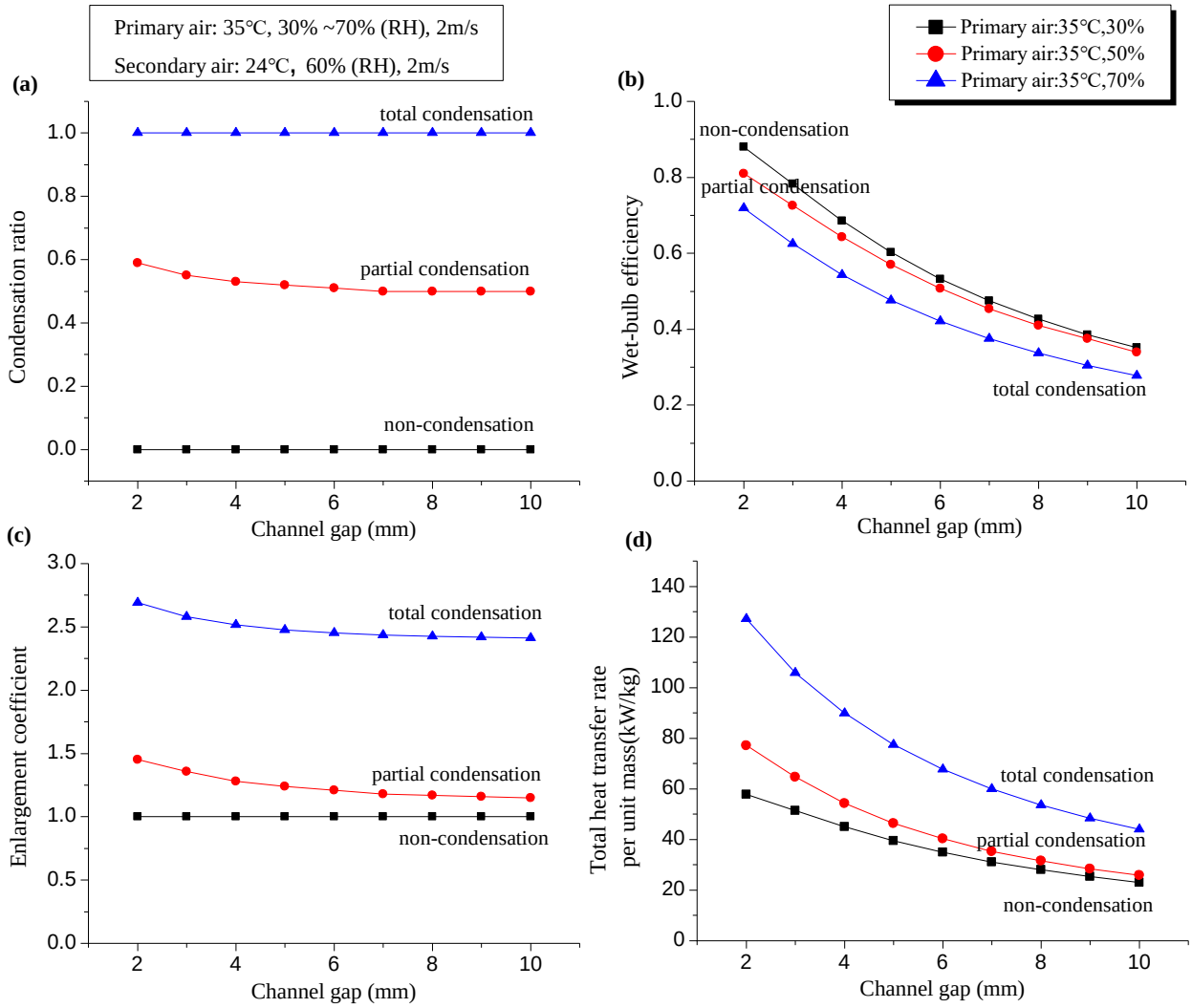

Fig.15 Influence of channel gap on: (a) condensation ratio; (b) wet-bulb efficiency; (c) enlargement coefficient; (d) total heat transfer rate per unit mass

Fig.15 presents the influence of channel gap on the thermal performance of IEC. Channel gap was found to be one of the most important influence factors of IEC performance without condensation in previous studies. In this study, the same conclusion is drawn for the condensation condition. It is observed that the increase of channel gap results in dramatic decreasing of the wet-bulb efficiency and total heat transfer rate. Meanwhile, the enlargement coefficient will also drop a little bit with the increase of channel gap. It is ascribed to the reason that the larger the channel gap, the more obviously the air bypasses, resulting in insufficient heat

exchange with the cold separated walls As the channel gap increases from 2mm to 10mm, the efficiency decreases from 88% to 35% under non-condensation state and from 72% to 28% under total condensation state.

It is noticed that the channel gap has more significant impact on the condensation state as the downswing trend of total heat transfer rate is more rapid compared with non-condensation state. It decreases dramatically from 57.8 kW/kg to 23.1 kW/kg under non-condensation state (60.0% decrease); from 77.1 kW/kg to 25.8 kW/kg under partial condensation state (66.5% decrease) and from 127 kW/kg to 44 kW/kg under total condensation state (65.4% decrease). It is owing to the fact that the increase of the channel gap not only weakens the sensible heat transfer but also impairs the condensation process, which can be validated by the condensation ratio and enlargement coefficient. The ratio declines especially when the channel gap is less than 5mm. So the total heat transfer rate and enlargement coefficient changes most greatly in this range. Considering this finding, the optimal channel gap should be no more than 5mm when there is condensation takes place.

5.2.8 Influence of wettability

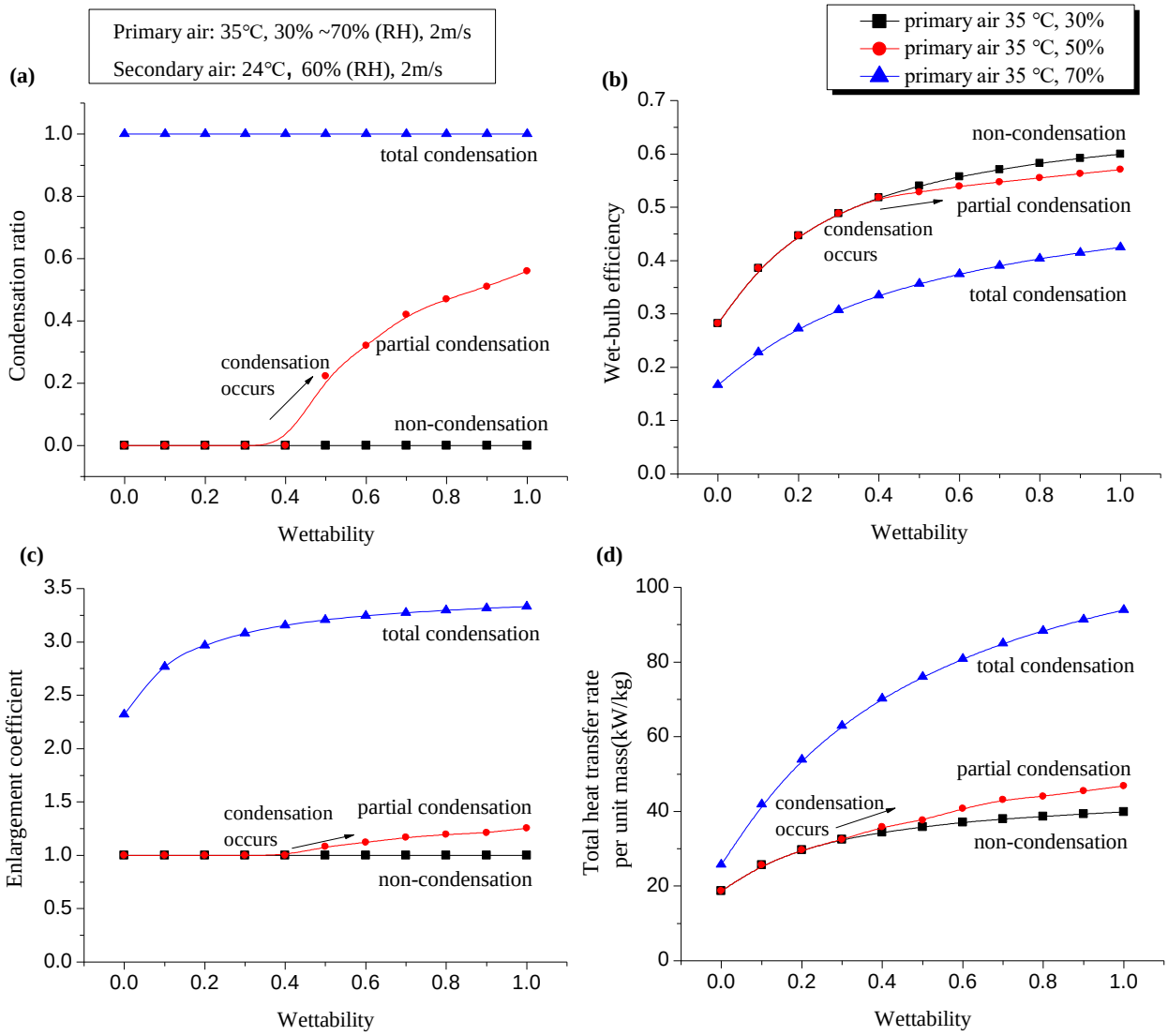

Fig.16 Influence of wettability on: (a) condensation ratio; (b) wet-bulb efficiency; (c) enlargement coefficient; (d) total heat transfer rate per unit mass

Fig.16 presents the influence of wettability on the thermal performance of IEC. It has been shown in previous studies that improving the wettability of secondary air channel are an effective measure to enhance the IEC efficiency. The reason is that the higher wettability increases the wet surface area for evaporation and reduced the wall temperature. In present study, improving the wettability is also found to have positive effect on increasing the wet-bulb efficiency and total heat transfer rate for both non-condensation and condensation states. In addition, the improvement of wettability can also change the IEC operation condition. It is found that the

condensation ratio increases from 0 to 0.58 when the wettability improves from 0 to 1.0 for the case of t_p=35℃, RH_p=50%.

However, the trends for wet-bulb efficiency and total heat transfer rate improvement for non-condensation and condensation states are slightly different. For non-condensation state, both of the indexes improve most significantly at the beginning when the wettability increases from 0 to 0.4 and slows down when the wettability exceeds 0.4. While for condensation sate, the overall increase trend of wet-bulb efficiency is relatively smoother and the improvement of total heat transfer is still significant when the wettability keeps increasing (although slower than trend at the beginning). It is attributed to that the increase of wettability improve both the heat transfer rate and mass transfer rate, but the heat transfer rate is counteracted a little because of the wall temperature rise brought by the condensation. The enhancement of mass transfer is embodied in the increase of enlargement coefficient. Considering this finding, the increase of wettability may bring even better benefit for IEC performance under condensation state.

5.2.9 Influence of cooler height

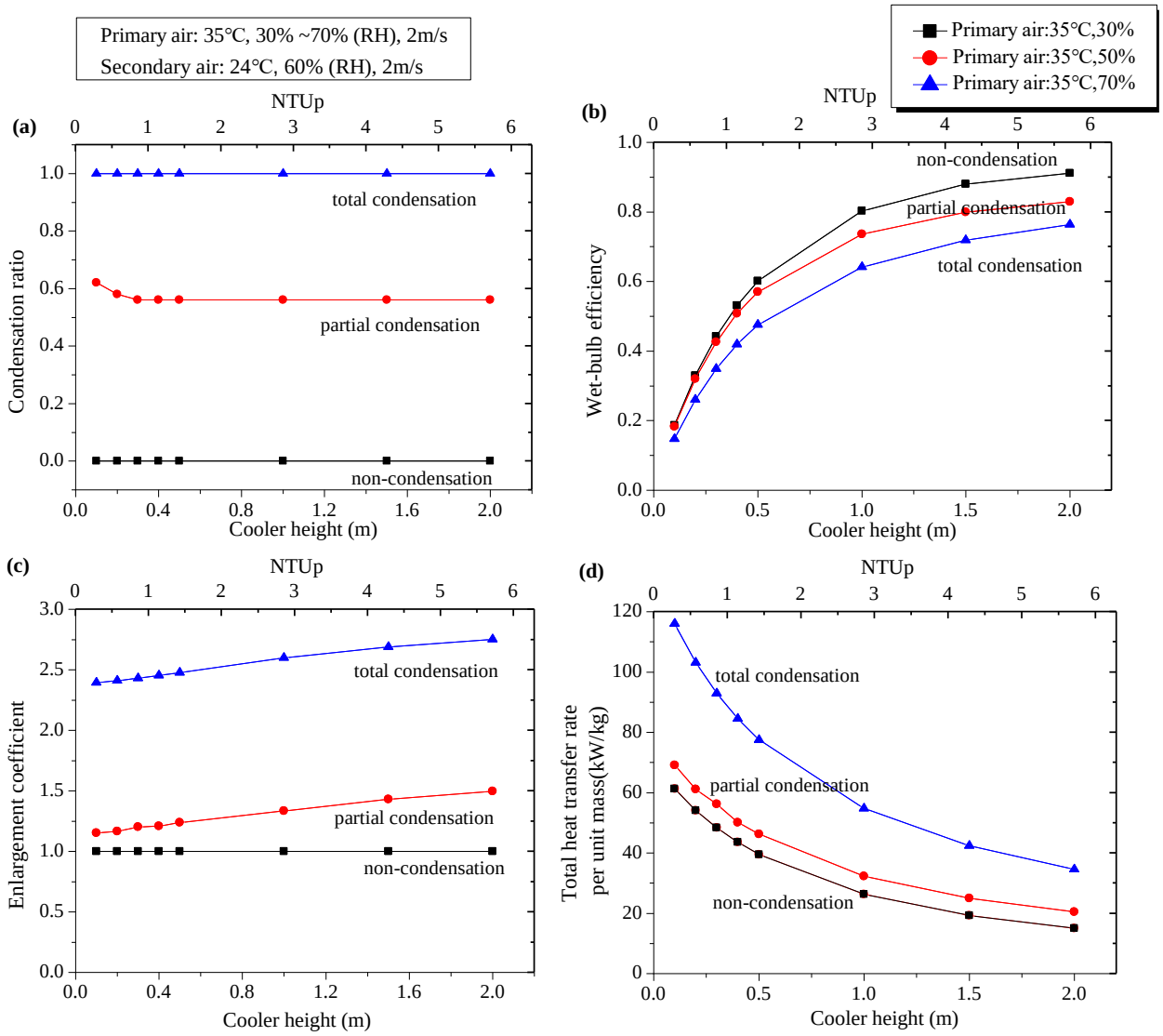

Fig.17 Influence of cooler height on: (a) condensation ratio; (b) wet-bulb efficiency; (c) enlargement coefficient; (d) total heat transfer rate per unit mass

Fig.17 presents the influence of cooler height on the thermal performance of IEC. The increase of cooler height results in larger heat transfer area and NTU. It improves the wet-bulb efficiency and the enlargement coefficient for condensation state. The trends of wet-bulb efficiency improvement with the increase of NTU under three operation states are similar. It improves very significantly when the NTU is less than 1.5 and slows down greatly once the NTU exceeds 3.0. So the IEC manufactory should compromise the cost and benefit. The total heat transfer rate is

found to decrease with the increase of NTU because this evaluation index takes the air mass into consideration. The improvement of heat transfer amount can not make up the adding of air mass inside the device so that the total heat gained by per unit mass is lowered.

6. Conclusion

This paper established a novel numerical model of indirect evaporative cooler (IEC) considering condensation from primary air. The influences of nine parameters were analyzed under three IEC operation states (non-condensation, partial condensation and total condensation) by using four evaluation indexes: condensation ratio, wet-bulb efficiency, enlargement coefficient and total heat transfer rate. The main results are highlighted as follows:

1) Compared with the other simulation results, the developed numerical model of IEC can predict the outlet primary air temperature and humidity with the discrepancy of 5.9% and 2.4%, respectively. The discrepancies for predicting the sensible, latent and total heat transfer rate on primary air side are 17.0%, 7.9% and 10.9%., respectively. The discrepancy can be attributed to different heat and mass transfer theory adopted, in which convection mass transfer model and heat and mass analogy theory was used for present model, while Fick's penetration theory was used in literature's model.

2) The condensation from primary air can raise the wall temperature and lower the wet-bulb efficiency of IEC, but the total heat transfer rate is improved because of the combined sensible heat transfer and dehumidification processes. The wet-bulb efficiency drops by 22% as the primary air RH increases from 30% to 90% (t_p=35℃, t_s=24℃, RH_s=60%), but the total heat transfer ratio is 1.8 times larger than that of non-condensation state when the RH reaches 90%.

3) The condensation from primary air tends to take place with higher primary humidity, smaller primary air velocity, lower secondary air temperature and humidity, higher secondary velocity, smaller channel gap and higher wettability. The stronger the condensation effect, the lower the wet-bulb efficiency is, but the higher the enlargement coefficient and total heat

transfer rate are. The enlargement coefficient can reach up to 4.5, implying the latent heat transfer accounts for 77.8% of the total heat transfer.

4) For the IEC condensation state, the increase of secondary air velocity, decrease of channel gap and improvement of wettability can achieve more obvious positive effect on enhancing the heat and mass transfer of IEC than in non-condensation state. In condensation sate, the wet-bulb efficiency and total heat transfer rate still increase significantly when the flow rate ratio of secondary air to primary air exceeds 1.5; the total heat transfer rate increases most rapidly when the channel gap is less than 5mm, so the optimal gap should be no more than 5mm; the total heat transfer rate still increases obviously when the wettability is more than 0.4.

Acknowledgement

This research is financially supported by the Public Housing Authority of the Hong Kong SAR Government and the Research Institute for Sustainable Urban Development (RISUD) of The Hong Kong Polytechnic University.

References

[1] Hanby, V. I., & Smith, S. T. (2012). Simulation of the future performance of low-energy evaporative cooling systems using UKCP09 climate projections. Building and Environment, 55, 110-116.

[2] Bravo, G., & González, E. (2013). Thermal comfort in naturally ventilated spaces and under indirect evaporative passive cooling conditions in hot–humid climate. Energy and Buildings, 63, 79-86.

[3] Smith, S. T., Hanby, V. I., & Harpham, C. (2011). A probabilistic analysis of the future potential of evaporative cooling systems in a temperate climate. Energy and Buildings, 43(2), 507-516.

[4] Khandelwal, A., Talukdar, P., & Jain, S. (2011). Energy savings in a building using regenerative evaporative cooling. Energy and Buildings, 43(2), 581-591.

[5] Campaniço, H., Soares, P. M., Hollmuller, P., & Cardoso, R. M. (2016). Climatic cooling potential and building cooling demand savings: High resolution spatiotemporal analysis of direct ventilation and evaporative cooling for the Iberian Peninsula. Renewable Energy, 85, 766-776.

[6] Liu, Z., Allen, W., & Modera, M. (2013). Simplified thermal modeling of indirect evaporative heat exchangers. HVAC&R Research, 19(3), 257-267.

[7] Krüger, E., González Cruz, E., & Givoni, B. (2010). Effectiveness of indirect evaporative cooling and thermal mass in a hot arid climate. Building and Environment, 45(6), 1422-1433.

[8] Jaber, S., & Ajib, S. (2011). Evaporative cooling as an efficient system in Mediterranean region. Applied Thermal Engineering, 31(14), 2590-2596.

[9] Bajwa, M., Aksugur, E., & Al-Otaibi, G. (1993). The potential of the evaporative cooling techniques in the gulf region of the Kingdom of Saudi Arabia. Renewable energy, 3(1), 15-29.

[10] Costelloe, B., & Finn, D. (2007). Thermal effectiveness characteristics of low approach indirect evaporative cooling systems in buildings. Energy and Buildings, 39(12), 1235-1243.

[11] Cruz, E. G., & Krüger, E. (2015). Evaluating the potential of an indirect evaporative passive cooling system for Brazilian dwellings. Building and Environment, 87, 265-273.

[12] El-Refaie, M. F., & Kaseb, S. (2009). Speculation in the feasibility of evaporative cooling. Building and Environment, 44(4), 826-838.

[13] Maclaine-Cross, I. L., & Banks, P. J. (1981). A general theory of wet surface heat exchangers and its application to regenerative evaporative cooling. Journal of heat transfer, 103(3), 579-585.

[14] Erens, P. J., & Dreyer, A. A. (1993). Modelling of indirect evaporative air coolers. International journal of heat and mass transfer, 36(1), 17-26.

[15] San Jose Alonso, J. F., Martínez, F. J., Gomez, E. V., & Plasencia, M. A. (1998). Simulation model of an indirect evaporative cooler. Energy and buildings, 29(1), 23-27.

[16] Chengqin, R., & Hongxing, Y. (2006). An analytical model for the heat and mass transfer processes in indirect evaporative cooling with parallel/counter flow configurations. International journal of heat and mass transfer, 49(3), 617-627.

[17] Hasan, A. (2012). Going below the wet-bulb temperature by indirect evaporative cooling: Analysis using a modified ε-NTU method. Applied Energy, 89(1), 237-245.

[18] Stabat, P., & Marchio, D. (2004). Simplified model for indirect-contact evaporative cooling-tower behaviour. Applied Energy, 78(4), 433-451.

[19] Liu, Z., Allen, W., & Modera, M. (2013). Simplified thermal modeling of indirect evaporative heat exchangers. HVAC&R Research, 19(3), 257-267.

[20] Kim, M. H., Jeong, D. S., & Jeong, J. W. (2015). Practical thermal performance correlations for a wet-coil indirect evaporative cooler. Energy and Buildings, 96, 285-298.

[21] Chengqin, R., Nianping, L., & Guangfa, T. (2002). Principles of exergy analysis in HVAC and evaluation of evaporative cooling schemes. Building and environment, 37(11), 1045-1055.

[22] Guo, X. C., & Zhao, T. S. (1998). A parametric study of an indirect evaporative air cooler. International communications in heat and mass transfer, 25(2), 217-226.

[23] Hettiarachchi, H. D., Golubovic, M., & Worek, W. M. (2007). The effect of longitudinal heat conduction in cross flow indirect evaporative air coolers. Applied Thermal Engineering, 27(11), 1841-1848.

[24] Riangvilaikul, B., & Kumar, S. (2010). Numerical study of a novel dew point evaporative cooling system. Energy and Buildings, 42(11), 2241-2250.

[25] Cui, X., Chua, K. J., & Yang, W. M. (2014). Numerical simulation of a novel energy-efficient dew-point evaporative air cooler. Applied Energy, 136, 979-988.

[26] Cui, X., Chua, K. J., Yang, W. M., Ng, K. C., Thu, K., & Nguyen, V. T. (2014). Studying the performance of an improved dew-point evaporative design for cooling application. Applied Thermal Engineering, 63(2), 624-633.

[27] Heidarinejad, G., & Moshari, S. (2015). Novel modeling of an indirect evaporative cooling system with cross-flow configuration. Energy and Buildings, 92, 351-362.

[28] Anisimov, S., & Pandelidis, D. (2015). Theoretical study of the basic cycles for indirect evaporative air cooling. International Journal of Heat and Mass Transfer, 84, 974-989.

[29] Zhao, X., Liu, S., & Riffat, S. B. (2008). Comparative study of heat and mass exchanging materials for indirect evaporative cooling systems. Building and Environment, 43(11), 1902-1911.

[30] Jain, D. (2007). Development and testing of two-stage evaporative cooler. Building and Environment, 42(7), 2549-2554.

[31] Heidarinejad, G., Bozorgmehr, M., Delfani, S., & Esmaeelian, J. (2009). Experimental investigation of two-stage indirect/direct evaporative cooling system in various climatic conditions. Building and Environment, 44(10), 2073-2079.

[32] Anisimov, S., Pandelidis, D., & Jedlikowski, A. (2015). Performance study of the indirect evaporative air cooler and heat recovery exchanger in air conditioning system during the summer and winter operation. Energy, 89, 205-225.

[33] La, D., Dai, Y., Li, Y., Ge, T., & Wang, R. (2010). Study on a novel thermally driven air conditioning system with desiccant dehumidification and regenerative evaporative cooling. Building and Environment, 45(11), 2473-2484.

[34] McKenzie, E. R., Pistochini, T. E., Loge, F. J., & Modera, M. P. (2013). An investigation of coupling evaporative cooling and decentralized graywater treatment in the residential sector. Building and Environment, 68, 215-224.

[35] Heidarinejad, G., Khalajzadeh, V., & Delfani, S. (2010). Performance analysis of a ground-assisted direct evaporative cooling air conditioner. Building and Environment, 45(11), 2421-2429.

[36] Kim, M. H., Park, J. Y., Ham, S. W., & Jeong, J. W. (2015). Energy conservation benefit of water-side free cooling in a liquid desiccant and evaporative cooling-assisted 100% outdoor air system. Energy and Buildings, 104, 302-315.

[37] Gao, W., Worek, W., Konduru, V., & Adensin, K. (2015). Numerical study on performance of a desiccant cooling system with indirect evaporative cooler. Energy and Buildings, 86, 16-24.

[38] Chen PL, Qin H, Huang YJ, Wu H, Blumstein C. The energy-saving potential of precooling incoming outdoor air by indirect evaporative cooling. ASHRAE Trans 1993;99(Pt 1).

[39] Delfani, S., Esmaeelian, J., Pasdarshahri, H., & Karami, M. (2010). Energy saving potential of an indirect evaporative cooler as a pre-cooling unit for mechanical cooling systems in Iran. Energy and Buildings, 42(11), 2169-2176.

[40] Cianfrini, C., Corcione, M., Habib, E., & Quintino, A. (2014). Energy performance of air-conditioning systems using an indirect evaporative cooling combined with a cooling/reheating treatment. Energy and Buildings, 69, 490-497.

[41] Jain, V., Mullick, S. C., & Kandpal, T. C. (2012). A financial feasibility evaluation of using evaporative cooling with air-conditioning (in hybrid mode) in commercial buildings in India. Energy for Sustainable Development.

[42] Guo, X. C., & Zhao, T. S. (1998). A parametric study of an indirect evaporative air cooler. International communications in heat and mass transfer, 25(2), 217-226.

[43] Zhan, C., Zhao, X., Smith, S., & Riffat, S. B. (2011). Numerical study of a M-cycle cross-flow heat exchanger for indirect evaporative cooling. Building and Environment, 46(3), 657-668.

[44] Lee, J., & Lee, D. Y. (2013). Experimental study of a counter flow regenerative evaporative cooler with finned channels. International Journal of Heat and Mass Transfer, 65, 173-179.

[45]https://www.thermalfluidscentral.org/encyclopedia/index.php/Thermally_developing_laminar_flow

[46] ASHRAE. Fundamentals, American Society of Heating, Refrigeration and Air Conditioning Engineers, USA; 1997.

[47] ASHRAE Handbook: Fundamentals. Mass transfer, Atlanta, GA; 2005. p. 9 (Ch.5).

[48] Huang, C. C., Yan, W. M., & Jang, J. H. (2005). Laminar mixed convection heat and mass transfer in vertical rectangular ducts with film evaporation and condensation. International journal of heat and mass transfer, 48(9), 1772-1784.

[49] Duan, Z., Zhan, C., Zhang, X., Mustafa, M., Zhao, X., Alimohammadisagvand, B., & Hasan, A. (2012). Indirect evaporative cooling: Past, present and future potentials. Renewable and Sustainable Energy Reviews, 16(9), 6823-6850.

[50] Cui, X., Chua, K. J., Islam, M. R., & Ng, K. C. (2015). Performance evaluation of an indirect pre-cooling evaporative heat exchanger operating in hot and humid climate. Energy Conversion and Management, 102, 140-150.